UiT The Arctic University of Norway

Faculty of Science and Technology
Department of Physics and Technology

Oceanographic variability and change in two fjords in northern Norway

Elena Bjørndalen

FYS-3900: Master's thesis in physics - 60 ECTS
June 2023

Contents

List of Figures

List of Tables

Abstract

Long-term hydrographic time series data from two fixed stations in the northern Norwegian fjords Malangen and Balsfjorden from the period 1980 - 2022 have been examined. The data have been supplemented with model results from the ocean model NorFjords160 over the period April 1st 2017 to December 31st 2022. To gain a deeper understanding of the oceanographic variability and change, the environmental drivers wind, precipitation and air temperature from the nearby weather stations Hekkingen fyr (Malangen) and Tromsø (Balsfjorden) and river runoff from the major rivers discharging in the fjords, Målselva (Malangen) and Nordkjoselva (Balsfjorden), have been examined for the same period. Additionally, for the years 2017 - 2022, particle tracking simulations have been used to investigate surface currents and the spread of particles from Målselva and Nordkjoselva.

The findings reveal statistically significant, positive air temperature trends at both Hekkingen fyr and Tromsø (up to 2.2 ^oC in autumn over the period 1980 - 2022). There is found seasonal variations in precipitation, however there are no discernible trends in river runoff at either locations. For the hydrographic conditions, the findings reveal statistically significant, positive temperature trends for both the surface layer (0.03 - 0.06 $^o\mathrm{C\,yr^{-1}}$ in Malangen and 0.04 - 0.07 $^o\mathrm{C\,yr^{-1}}$ in Balsfjorden) and deep layers (0.03 - 0.04 $^o\mathrm{C\,yr^{-1}}$ in Malangen and 0.01 - 0.04 $^o\mathrm{C\,yr^{-1}}$ in Balsfjorden) throughout all four seasons, in both fjords. There are no statistically significant trends regarding deep layer salinity in Malangen, whereas in Balsfjorden there is a statistically significant, negative trend in the spring and summer surface layers, as well as the summer deep layer. I hypothesize that the changes in temperature are linked to warming of the coastal water masses observed over the same period (Albretsen et al., 2011a; IMR, 2023), and the observed increase in air temperature. During the study period the surface CW has gotten fresher, while the deep CW has gotten more saline (Albretsen et al., 2011a; IMR, 2023). However, the changes in salinity in the fjords are less pronounced. The negative slopes of the estimated surface salinity trends may indicate an impact of freshening CW combined with a "normal" runoff pattern. For the deep layer, effective downward mixing of freshwater, changes in the frequency of AW inflow and the closeness of the stations to the river mouth versus the fjord mouth are presented as possible

reasons as to why the signal from the coast is not visible in the fjords.

The particle tracking simulations reveal that particles suspended from Målselva are transported far along the coast into the fjords and sounds north of Tromsø, while particles suspended from Nordkjoselva mainly stay in Balsfjorden. Further it is found that runoff from Målselva, which has a far higher water transport compared to Nordkjoselva, is not a source of (relatively) fresh water to Balsfjorden, but supplies relatively fresh water to the coastal area.

Acknowledgements

Firstly, I would like to thank my supervisors, Jofrid Skarðhamar and Angelika Renner, for always having open doors and for valuable feedback and discussions. The time and effort you have put into me and this thesis is greatly appreciated, and I am glad that my somewhat arbitrary outreach to IMR led me to you two!

Thank you to Johanne and Julie for listening to both my breakthroughs and breakdowns, with equal patience. You have been the best distractions.

Further, I would like to thank Pål Næverlid Sævik at IMR, Bergen for valuable help with data processing. You may or may not, to a small group of people who also happen to be my closest friends, be known as "Python-Pål".

Thank you to my family and friends for believing in me when I had no idea what I was doing. And lastly, thank you to Jarl Henning. You have been more supportive than no man has ever been, I am sure of it.

Elena Bjørndalen
Tromsø, 29.05.2023

1

Introduction

Fjords are complex systems, influenced by both the ocean and the atmosphere, and although they share some common characteristics, they are also highly diverse. The depth, width and surrounding topography will vary from fjord to fjord, so that the hydrography and dynamics of one fjord may not necessarily be applicable to another. The hydrographic and dynamic conditions in fjords can impact the marine ecosystem in several ways, such as nutrient distribution and the abundance of marine organisms. Understanding the physical oceanography and the processes unique to each fjord is crucial in order to predict this fjord's impact on its marine ecosystem, its capacity to endure e.g., fish farming or river regulations, and to predict the response to both natural and anthropogenic changes.

Hydrography refers to the physical features of the water, such as temperature, salinity and density, and how they vary with depth, space and time. The study of hydrography includes water mass properties, circulation patterns and water exchange between the fjord and the coast. Dynamics meanwhile refers to the physical processes that drive water motion and mixing, where examples of such physical processes can be winds, freshwater input from rivers and tides.

The aim of this thesis is to investigate the interannual and seasonal variability of the physical oceanography in two adjacent fjords in northern Norway, with the primary focus on the surface layer. The study period spans from 1980 to 2022, as the available historical data is most consistent from 1980 and onwards. The hydrographic variability is discussed against external forcing such as river

runoff, wind, precipitation and air temperature. Additionally, particle tracking simulations are used to examine the transport and dispersion of particles in the surface layer, and the role that oceanographic processes play in shaping the particle distribution. By examining these aspects, the study aims to provide a deeper understanding of the long-term variability of oceanographic conditions and possible impacts on passive tracers such as nutrients, dissolved material or phytoplankton in northern Norwegian fjords.

1.1 Physical processes in fjords

A fjord is a glacially-cut structure, situated at high latitudes (Inall and Gillibrand, 2010). In most fjords, there is a topographical barrier, a sill, at the entrance (Aksnes et al., 2019). The entrance of the fjord is often called the mouth. Fjords are highly diverse; sills may vary in depth and number and, for some fjords, shallow coastal plateaus may serve as the sill. Furthermore, how connected the fjord is to the coast can vary from a relatively open connection to more land-locked characteristics. Fjords have a high supply of freshwater (Inall and Gillibrand, 2010). For the fjords on the Norwegian mainland, the supply of freshwater mostly stems from river runoff, discharging in the inner part, called the head. While for e.g. fjords in the Norwegian Arctic archipelago of Svalbard the main supply of freshwater is tide-water glaciers terminating at the head (Halbach et al., 2019).

In sill-fjords, the water column can theoretically be divided into three distinct layers (Fig. 1.1) (Farmer and Freeland, 1983). The surface layer comprises relatively fresh water, which is a result of freshwater input from rivers and in the case of Arctic fjords, glacial melt water (Cottier et al., 2010). The thickness of this layer is typically in the range of 1 to 5 m (Aksnes et al., 2019). Below the surface layer and down to sill depth sits the intermediate layer. In fjords with shallow sills, this layer may be absent, while in fjords with deep sills it may be many tens of meters thick (Inall and Gillibrand, 2010). The hydrographic properties of the intermediate water masses depend on the coastal water at a corresponding depth outside the fjord. With a slight phase-delay, the intermediate water mirrors the stratification of the coastal water (Stigebrandt, 2012). The area below sill depth is known as the deep layer. The water masses in this layer are variously referred to as basin water (Stigebrandt, 2012; Aksnes et al., 2019; Darelius, 2020) or deep water (Farmer and Freeland, 1983; Inall and Gillibrand, 2010); the former will be used in this thesis.

Fjords are subject to forcing both internal and external to the fjord system. Driving mechanisms internal to the fjord system are freshwater runoff, local winds and tides. Driving mechanisms external to the fjord system are for example

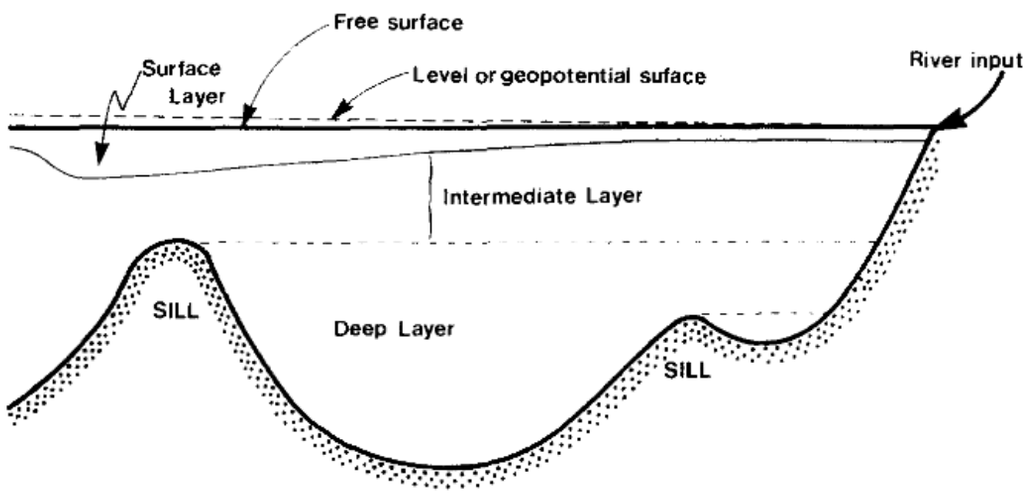

Figure 1.1: Schematic depicting the typical layering in a sill fjord. From Farmer and Freeland (1983).

temporal variations of sea level and density in the coastal water (Stigebrandt, 2010). Variations in sea level at the coast may be induced by tides, or meteorological phenomena such as storm surges or passing pressure systems (Inall and Gillibrand, 2010). Variations in density may occur due to non-local winds which induce coastal up- or downwelling, advection of different water masses (Sætre, 2007) or seasonal changes.

Most fjords have one or more rivers discharging into them, most often at the head. The freshwater runoff at the inner part of the fjord gives rise to a density driven current flowing out of the fjord. Wind-induced mixing entrains the underlying, more saline water into the outflowing surface current and in accordance with volume conservation, a compensating current containing coastal water directed inward is set up beneath the outflowing surface current (Inall and Gillibrand, 2010). This circulation pattern is called estuarine circulation and is a dynamic response to the internal forcing of freshwater discharge to the fjord (Fig. 1.2). While estuarine circulation contributes to water exchange between the fjord and the coast, the contribution is rather small. The dominating mode for water exchange is the intermediary exchange (Aure et al., 1996), which is a result of the external forcing from density and sea level fluctuations at the coast.

Vertical density variations in the coastal water caused by wind-induced coastal up- or downwelling give rise to horizontal pressure gradients between the fjord and the coast (Stigebrandt, 2012). In the case of a narrow fjord, these horizontal pressure gradients drive currents through the mouth, directed either into or

out of the fjord. If the fjord is wider than the Rossby radius of deformation, a so-called broad fjord (Cushman-Roisin et al., 1994), the movement may be influenced by the Earths rotation. The effects of rotation and the concept of narrow and broad fjords are described in further detail in Appendix. 6.1.

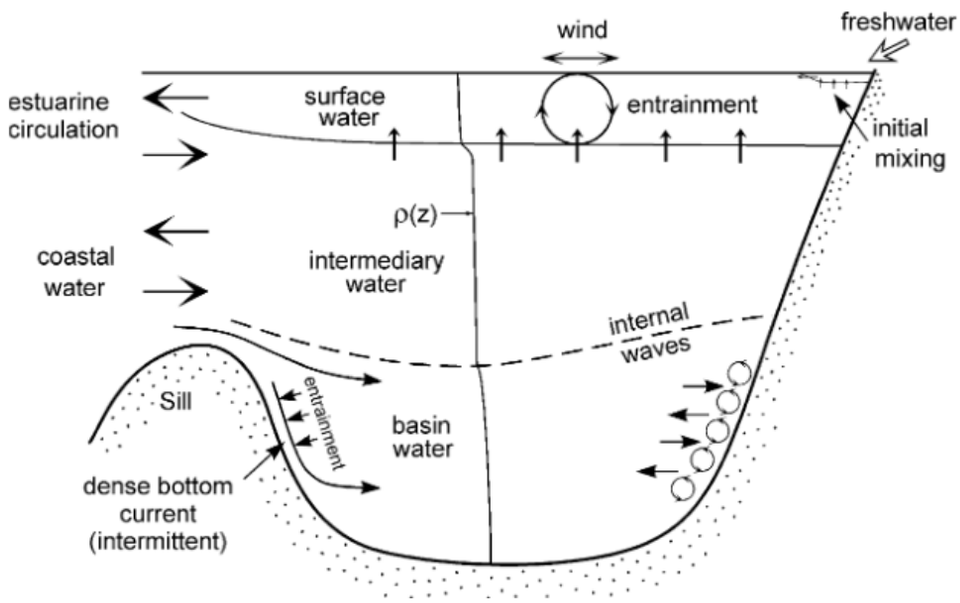

Figure 1.2: Schematic depicting the typical water masses comprised to each layer, and the processes affecting them. From Stigebrandt (2012).

The submarine sill(s) act as a topographic barrier, isolating the basin water from the coastal water (Stigebrandt, 2012; Darelius, 2020). However, if water of sufficient density is aspirated over the sill, a so called deep water renewal may take place. Renewal of the basin water may either be partial or full. A partial renewal is when the aspirated water is dense enough to displace some of the water beneath the intermediate layer, but not a sufficient amount of basin water. A full renewal has occurred when the resident basin water is displaced upwards, and replaced by aspirated, dense coastal water. This happens when the density of the aspirated water is greater than the maximum density of the basin water (Inall and Gillibrand, 2010; Edwards and Edelsten, 1977; Gade and Edwards, 1980; Allen and Simpson, 1998). In stagnant periods, the density of the basin water is continuously being reduced due to diapycnal mixing, laying the groundwork for quasi-periodic renewal (Stigebrandt, 2012; Inall and Gillibrand, 2010). Weak mixing can lead to longer stagnation periods, which in turn can lead to hypoxia or anoxia due to oxygen decline from microbial consumption (Aksnes et al., 2019).

2

Data and Methods

2.1 Study area

2.1.1 Coastal water masses

Along the Norwegian coast, the main water masses are of coastal and Atlantic origin (Skarðhamar and Svendsen, 2005). Originating in the Baltic Ocean and modified by river runoff along the coast, the Norwegian Coastal Current (NCC) is a northward flowing, wedge-shaped, low-salinity current (Mitchelson-Jacob and Sundby, 2001). The NCC influences the coastal area and fjords all along the coast, and consists of relatively cold and low salinity water called Norwegian Coastal Water (NCW), hereafter CW (Skarðhamar and Svendsen, 2005).

The NCC flows northwards between the Norwegian coast and the Norwegian Atlantic Current (NwAC), which is an extension of the North Atlantic Current (NAC), transporting relatively warm and saline (>35 PSU) Atlantic Water (AW) northwards (Sætre, 2007; Skarðhamar and Svendsen, 2005; Helland-Hansen and Nansen, 1909). Due to mixing between the two currents, the salinity of the NCC increases while the salinity of the NwAC decreases on their journey northward (Mitchelson-Jacob and Sundby, 2001).

In spring and summer, when the freshwater runoff is at its maximum levels, the stratification in the upper part of the NCC is strong. The prevailing wind direction along the coast in summer is northerly, following Ekman transport leads to westward displacement of the low-salinity surface water, raising the

AW in the water column. Under certain conditions, this allows for inflow of AW to the fjords (Mitchelson-Jacob and Sundby, 2001; Sætre, 2007). During winter, the prevailing wind direction at the coast is southwesterly, and Ekman transport leads to a pile up of water along the coast. This induces downwelling, and the coastal wedge becomes narrow and deep (Mitchelson-Jacob and Sundby, 2001).

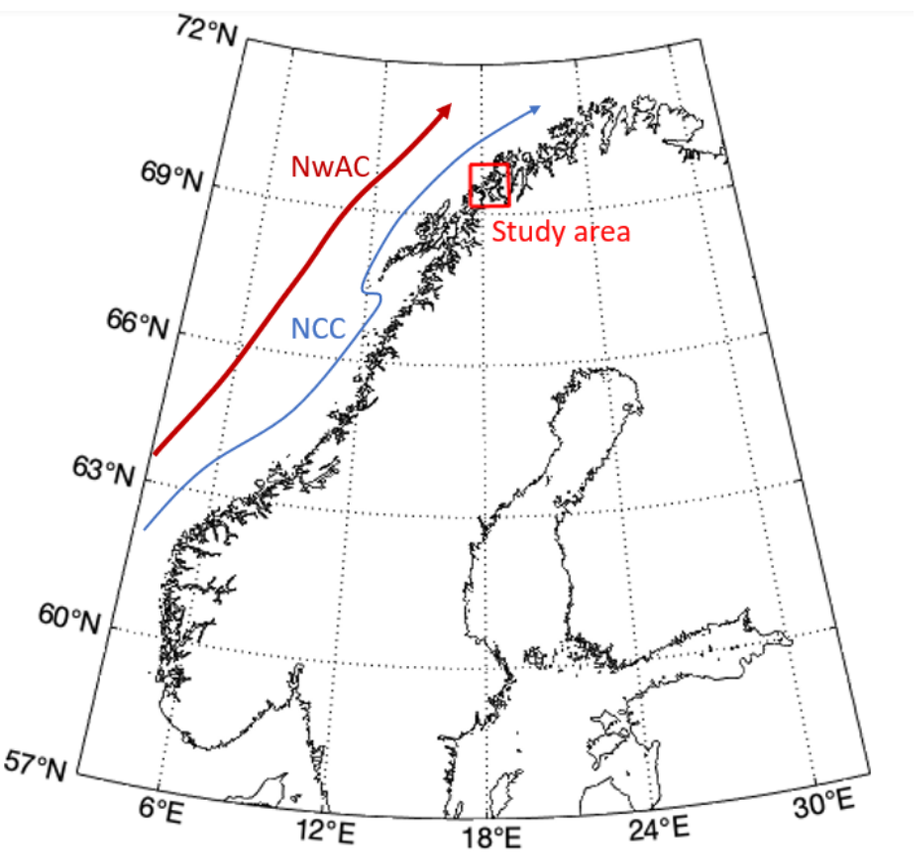

Figure 2.1: Schematic map showing the path of the NwAC (dark red) and NCC (blue) along the Norwegian coast. Red square indicates the study area for this thesis.

2.1.2 Malangen and Balsfjorden

Both Malangen and Balsfjorden are located in Troms county in Northern Norway (Fig. 2.2). From Hekkingen fyr at the fjord mouth to Nordfjordbotn at the fjord head, Malangen extends about 56 km. The fjord can be divided into two basins. The basins are separated by a sill area with varying bathymetry, but generally in a depth range of 150 - 160 m. The maximum depth of the outer basin is about 400 m, whereas the inner basin has a maximum depth of 250 m.

A few kilometres off the fjord mouth, there is a deep sill, measuring about 200 m, which separates the outer basin from the shelf area. Beyond the sill is the Malangen deep (Malangsdjupet), which reaches a maximum depth of approximately 400 m. The largest supply of freshwater to Malangen comes from the Målselva river, which discharges into the side fjord Målselvfjorden. Malangen is a broad fjord (around 6 km), where the circulation will be affected by the Earths rotation, and the surface circulation is mostly driven by the freshwater input (Rinde et al., 1998).

From the southern tip of Tromsøya (the island of Tromsø) at the fjord mouth to Nordkjosbotn at the fjord head, Balsfjorden stretches over about 59 km. It is separated from the open ocean by three relatively narrow sounds, Tromsøysundet, Sandessundet and Rystraumen. Their sill depths are approximately 8, 11 and 50 m, respectively. At the narrowest point, Tromsøysundet is about 537 m wide, Sandessundet is about 565 m wide, while Rystraumen is the widest at about 600 m. Tromsøysundet and Sandessundet are located on either side of Tromsøya, while Rystraumen connects Balsfjorden to Malangen. There are strong tidal currents in Rystraumen. The current changes direction approximately 25 minutes before high and low tide, and is directed eastward during rising tide and westward during falling tide (Statens kartverk Sjø, 2008). The outer part of Balsfjorden is relatively shallow, around 25 m, but gets gradually deeper towards the inner part. The deepest depth is about 187 m, and is located in the middle of the fjord. The freshwater supply comes from several small rivers, where the largest contribution is from Nordkjoselva, discharging at the head of the fjord. Balsfjorden is a narrow fjord (around 4 km), meaning the circulation may be affected by rotation, but to a far lesser extent than Malangen (Rinde et al., 1998).

All dimensions, in addition to geographical names, were obtained from Kartverket (Kartverket, 2023).

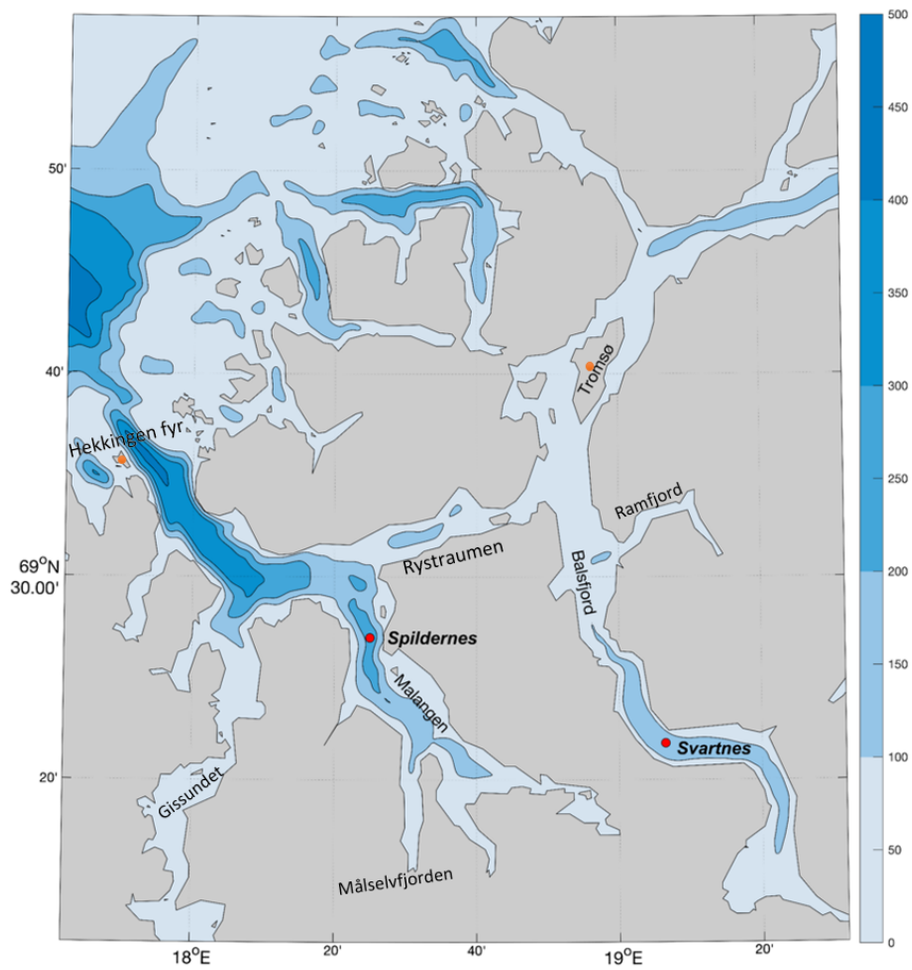

Figure 2.2: Bathymetric map of Malangen, Balsfjorden and the surrounding area. Red points are CTD stations, orange are weather stations. Colorbar representing depth (m)

2.2 Hydrographic data

A large part of this thesis has been to organize and compile existing historical data together with newly acquired data. The goal has been homogenous datasets of hydrographic measurements (conductivity, temperature and depth, CTD) from the two fjords Malangen and Balsfjorden. The data used in this thesis is a combination of data collected between 1980 and 2018 as part of the Havmiljødata (HMD) program organized by UiT The Arctic University of Norway, newer data collected by the Institute of Marine Research (IMR) as a part of regular coastal monitoring, and data collected during teaching cruises for the BIO-2516 Ocean Climate course at UiT.

One station in each fjord has been selected to describe changes and patterns over the time period. These stations are Spildernes in Malangen and Svartnes in Balsfjorden. Henceforth referred to as Malangen Spildernes and Balsfjord Svartnes, respectively. They have been chosen due to their locations being approximately mid-fjord, they are the deepest stations in their respective fjords, and have the largest data availability.

The conductivity data collected by IMR and UiT (HMD) had been calibrated against water samples, which had been analyzed at IMR Bergen and UiT, respectively (Mankettikkara, 2013). Data collected through the BIO-2516 course relied on factory calibration of the conductivity sensors. The CTD data were provided in various file formats, with files containing in-situ temperature, practical salinity and pressure/depth.

Practical salinity has been converted to absolute salinity, and conservative temperature was calculated from absolute salinity, in-situ temperature and sea pressure. The conversions were done using the Python implementation of the Gibbs SeaWater (GSW) Oceanographic Toolbox, following TEOS-10 standards (https://www.teos-10.org/).

The large size of the dataset and variable file formats from different ships and cruises presented a challenge in ensuring the accuracy of the measurements. An erroneous measurement was detected at Spildernes (Malangen) in May 1993, where registered salinity was at 17.5 $g\,kg^{-1}$ throughout the water column. The entire profile was removed from the analyses.

Due to significant seasonal variability (Fig. 2.3), it was found necessary to split the data into four seasons. To capture the warmest and coldest periods, and hence facilitate the detection of seasonal trends, the following definitions of seasons have been used: winter is defined as January to March, spring is April to June, summer is July to September, and autumn is October to December. Furthermore, when investigating trends, it was desirable to examine the surface- and the deep layer. Due to data availability and coverage, the depth to represent the surface layer was chosen to be 5-6 m in both fjords. By examining the vertical profiles of each CTD cast (not shown), it was possible to identify the deepest depth where measurements were taken most frequently. For Malangen Spildernes this depth is 200 m, while for Balsfjord Svartnes it is 140 m, hence the depth to represent the deep layer in Malangen is 200 m and the depth to represent the deep layer in Balsfjorden is 140 m.

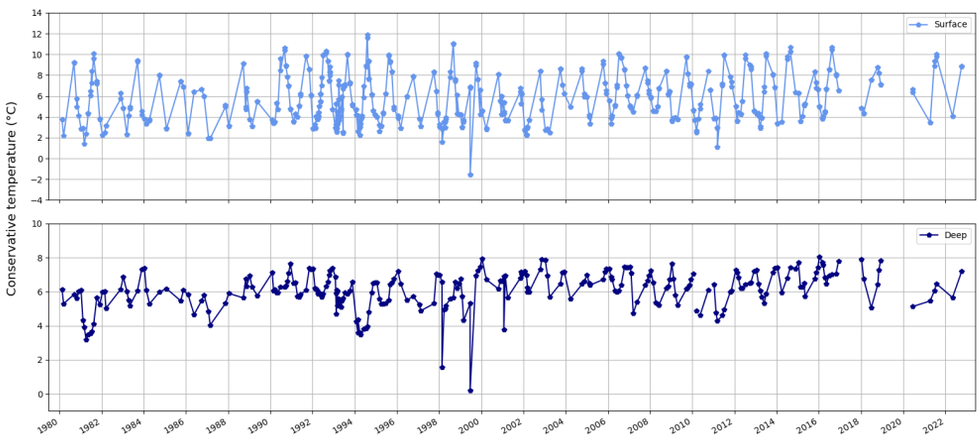

(a) Conservative temperature (^{o}C).

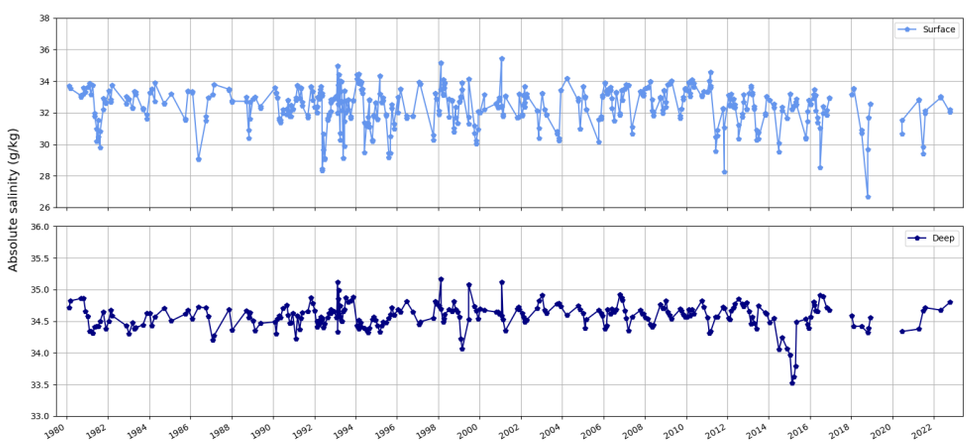

(b) Absolute salinity g kg^{-1} .

Figure 2.3: Interannual variability of conservative temperature (a) and absolute salinity (b) in the surface- (5-6 m) and deep layer (200 m) of Malangen Spildernes from 1980 - 2022.

2.3 Hydrographic model data

To fill inn for missing data and extend the time series, temperature and salinity data from the available model runs with the ocean model NorFjords160 were extracted at the locations of Spildernes and Svartnes over the period April 1st 2017 to December 31st 2022. Through comparison with observations, the model is found to successfully reproduce temperature and salinity in the fjords (Appendix. 6.2)

NorFjords160 is a high resolution model setup for Norwegian fjords. It reproduces currents, hydrography and water level using the open-source Regional Ocean Modelling System (ROMS) to numerically solve the primitive equations. ROMS is a state-of-the-art, free-surface, three dimensional, hydrostatic, primitive equation ocean model that uses generalized terrain-following s-coordinates in the vertical (Shchepetkin and McWilliams (2005), or see https://www.myroms.org/).

The horizontal resolution is 160 m x 160 m and there are 35 vertical levels, where the resolution is more dense in the upper part of the water column (Sandvik et al., 2019). In this study, we used available results from IMR's model archive for the domain A11, covering the fjords in Troms county, including Malangen and Balsfjorden (IMR, 2022). The atmospheric forcing is provided from AROME MetCoOp (Meteorological Co-operation on Operational Numerical Weather Prediction) 2.5, which is the main forecasting system at the Norwegian Meteorological Institute (Dalsøren et al., 2020; Müller et al., 2017). The forcing along the open boundaries was acquired from the coastal model NorKyst800, which has a horizontal resolution of 800 x 800 m (Albretsen et al., 2011b; Asplin et al., 2020; Albretsen et al., 2022). NorKyst800 covers the entire Norwegian coast and uses ROMS as well. Freshwater input is provided by the Norwegian Water Resources and Energy Directorate (NVE). Based on measured water flow, the total amount of runoff to each drainage area is estimated with a hydrological model (NVE - norges vassdrags- og energidirektorat, 2023).

Both the model systems NorKyst800 and NorFjords160 are set up for the entire Norwegian coast, with the best available and most realistic input data on bathymethry, meteorology, boundary forcing and runoff. For more information on the model systems, see e.g., Skarðhamar et al. (2018) or Dalsøren et al. (2020).

2.4 River runoff data

The analysis on river runoff is based on daily runoff data from Målselva and Nordkjoselva. These datasets, which serve as input for the model as explained

above, have been used to generate Hovmöller diagrams for the period January 1980 to late October 2022 (Fig. 3.7 & Fig. 3.8).

2.5 Particle tracking model

To gain insight on surface layer currents and their effect on the transport of suspended particles from Målselva and Nordkjoselva, the offline ocean particle tracking model LADiM (Lagrangian Advection and Diffusion Model) (Ådlandsvik, 2022) was used. LADiM was forced using current output from the NorFjords160 simulation. In our simulations, 50 particles were deployed at the mouths of Målselva and Nordkjoselva following the maximum spring runoff in the years 2017 - 2022 (Tab. 2.1). To cover the entire tidal cycle, particles were released at two high tides and two low tides on the day after maximum spring runoff. The particles had a fixed depth of 1 m, and the horizontal trajectories were tracked for 14 days, with hourly logging of position, temperature and salinity.

The output was used to generate trajectory maps which also display the surface salinity. The surface salinity is given in practical salinity unit (PSU). Furthermore, to get an overview of where the particles end up or accumulate, the study area was divided into four regions (Fig. 2.4). The four regions are Malangen, Balsfjorden, inshore and offshore (hereafter referred to as R1, R2, R3 and R4, respectively) and the percentage of particles originating from each river that ended up in each region was calculated.

Table 2.1: The date and corresponding maximum spring runoff (m^3s^{-1}) from each river, as well as the ratio between the two. The ratio is calculated by dividing the amount of runoff from Målselva by the amount of runoff from Nordskjoselva.

River	Date [dd.mm.YYYY]	Runoff (m^3s^{-1})	Ratio
Målselva	12.06.2017	1248.9	24.3
Nordkjoselva	11.06.2017	51.3	
Målselva	22.06.2018	824.5	19.6
Nordkjoselva	15.05.2018	42.1	
Målselva	08.06.2019	938.1	8.0
Nordkjoselva	24.04.2019	116.6	
Målselva	08.06.2020	1212.8	11.4
Nordkjoselva	02.06.2020	106	
Målselva	12.06.2021	1122.6	17.3
Nordkjoselva	12.06.2021	64.8	
Målselva	03.06.2022	1041.7	17.6
Nordkjoselva	27.05.2022	59.3	

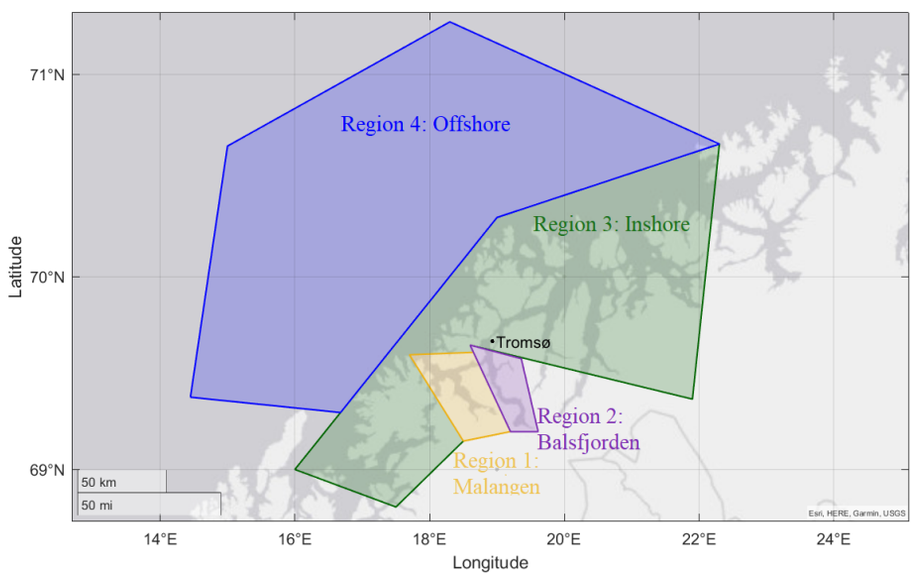

Figure 2.4: The study area was divided into four regions: Malangen, Balsfjorden, inshore, and offshore. The final percentage of particles that ended up in each region was then calculated.

2.6 Meteorological data

Wind, daily mean air temperature and daily precipitation data are provided by the Norwegian Meteorological Institute through seklima.met.no (accessed 09.02.2023). Hekkingen fyr weather station was used for Malangen, while Tromsø weather station was used for Balsfjorden, as they are the nearest and most representative weather stations to the respective fjords (Fig. 2.2).

From Tromsø weather station, wind, air temperature and precipitation data were extracted for the entire study period, January 1st 1980 - December 31st 2022. From Hekkingen fyr, wind and air temperature were retrieved for the full duration of the study period, while precipitation data was only retrieved from January 1st 1980 - December 30th 2004, due to lack of data after this date.

Both the air temperature and precipitation data were sorted by season, where the division of seasons is the same as for the hydrographic data. For air temperature, the seasonal mean for each year, in addition to the seasonal mean for the entire period, was calculated. For the precipitation data, the total seasonal precipitation (mm), defined as the sum of precipitation over a season, was calculated for each year, and further averaged over the entire period to derive the seasonal mean.

2.7 Statistical methods

For both the CTD- and Norfjords160 data, the seasonal mean temperature and salinity for each year was calculated, along with the standard deviation (std). The std describes the degree of variation within the data, where a small std indicates that the data points are close to the mean and variability is small, while a large std indicates that they are more spread out.

The std is represented as a shaded area around the mean in Figs. 3.9, 3.10, 3.11 and 3.12. The upper and lower limits of the shaded area were calculated as mean ± std. For some years, there is only one measurement over the months defined in the season, hence there is no std for these cases.

Visual inspection together with linear regression was used to investigate whether there has been a significant increase or decrease in seasonal temperature, salinity and air temperature during the study period. The method of linear regression applied is the ordinary least squares method (Groß, 2012) from the Python library statsmodels.

From linear regression, the most important statistical variables returned are the p-values and coefficients. In this study, if the p-value < 0.05, the results are said to be statistically significant because the parameter is then significant to a 95% confidence level. The mathematical relationship between the variables x and y is described by the coefficients, hence a positive coefficient indicates an positive (increasing) trend, while a negative coefficient indicates a negative (decreasing) trend.

To best capture trends, all regression lines were calculated from raw data, i.e., before the seasonal means were calculated. Furthermore, regression analyses of temperature and salinity were based solely on the CTD data, hence the NorFjords160 data was not included when estimating trends.

3

Results

3.1 Environmental conditions

Following is an overview of how the environmental conditions air temperature, wind, precipitation and river runoff have evolved over the study period, January 1st 1980 - December 31st 2022. The meteorological data representative for the Malangen area is from Hekkingen fyr weather station, located on the island Hekkinga off the mouth of Malangen, while the meteorological data representative for the Balsfjorden area is from Tromsø weather station, located at the top of Tromsøya (Fig. 2.2).

3.1.1 Wind

The prevailing wind direction at Hekkingen fyr is south-southeast. In the period 1980-2000, southerly winds also occurred frequently (Fig. 3.1). The prevailing south-southeasterly wind direction indicates topographic steering by the surrounding terrain and predominantly downfjord winds in Malangen. The most common wind speed is 8 - 10.7 ms^{-1}.

At the meteorological station in Tromsø, the prevailing wind direction is south-southwest and southerly for the entire period 1980-2022. As for Malangen, the wind direction here suggests topographic steering, with downfjord winds being the most frequent. The wind speed is slightly lower in Tromsø compared to Hekkingen, with the most common wind speed being 3.4 - 5.4 ms^{-1}.

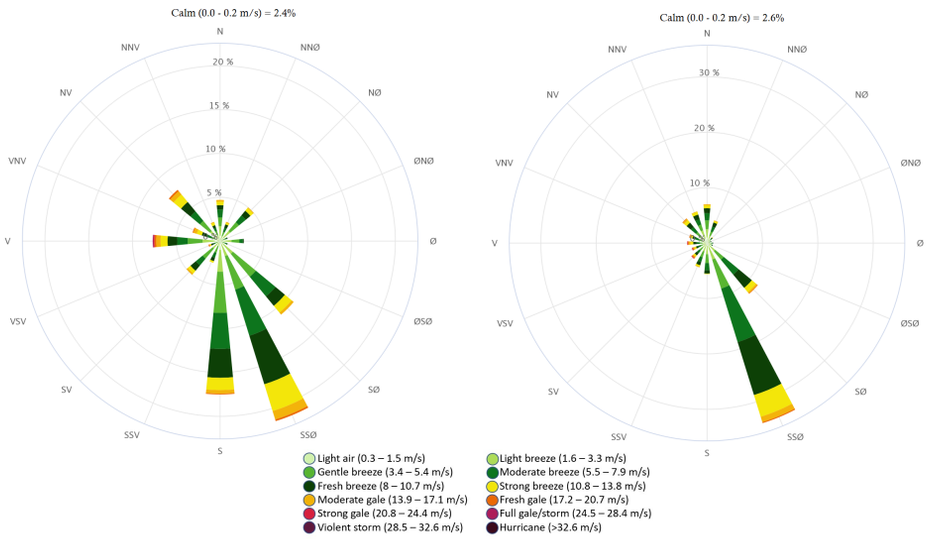

Figure 3.1: Wind roses show the frequency of wind speed by direction at Hekkingen fyr weather station fron January 1980 - December 2000 (left) and January 2001 - December 2022 (right). Figure created through the Norwegian Meteorological Institute (https://seklima.met.no/windrose/)

Figure 3.2: Wind roses show the frequency of wind speed by direction from the meteorological station Tromsø, from January 1980 - December 2000 (left) and January 2001 - December 2022 (right). Figure created through the Norwegian Meteorological Institute (https://seklima.met.no/windrose/)

3.1.2 Air temperature

The seasonal mean air temperature from Hekkingen fyr in the period 1980-2022 is -0.9, 5.7, 10.7 and 2.2 ^oC for winter, spring, summer and autumn, respectively (Tab. 3.1). For each season, there is found a statistically significant, positive air temperature trend over the same period (Fig. 3.3). The largest temperature increase is seen during autumn, with a temperature rise of approximately 2.2 ^oC over the observed period. Following is summer (1.3 ^oC), winter (0.97 ^oC) and lastly spring (0.94 ^oC).

The seasonal mean air temperature at Tromsø during the period 1980 - 2022 is -2.9, 5.1, 10.2 and 0.15 for winter, spring, summer and autumn, respectively (Tab. 3.1). Noticing it is slighly colder at Tromsø compared to Hekkingen fyr year round. Over the period there has been a statistically significant, positive trend for all four seasons (Fig. 3.4). With an increase of approximately 2.2 ^oC, autumn is the season with the largest observed temperature increase at Tromsø weather station as well. Following is summer (1.6 ^oC), spring (1.3 ^oC) and lastly winter (0.9 ^oC).

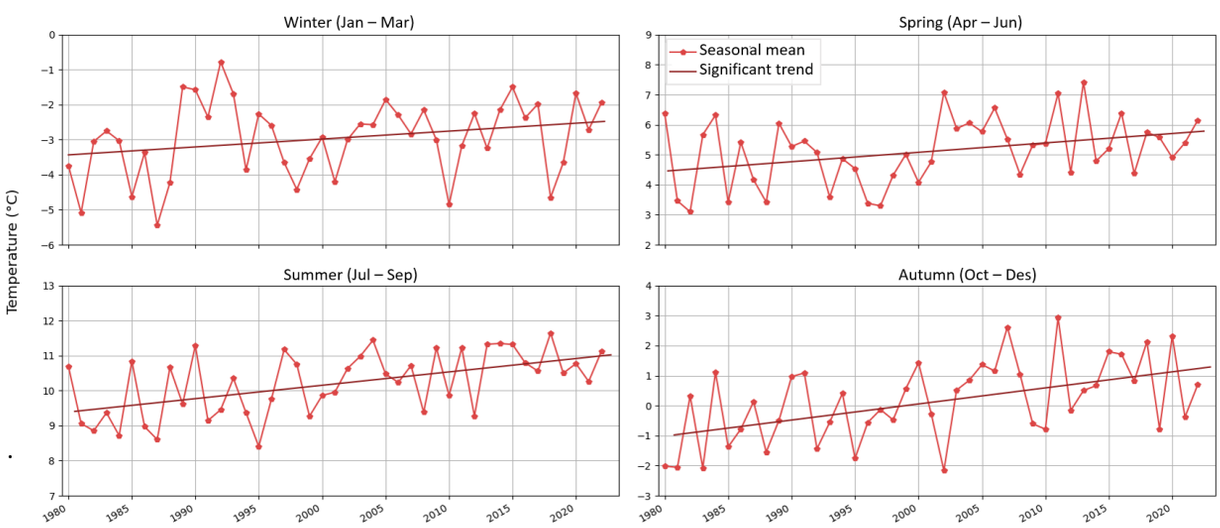

Figure 3.3: Seasonal mean air temperature (^oC) from Hekkingen fyr weather station. Solid lines indicate statistically significant trend ($p < 0.05$).

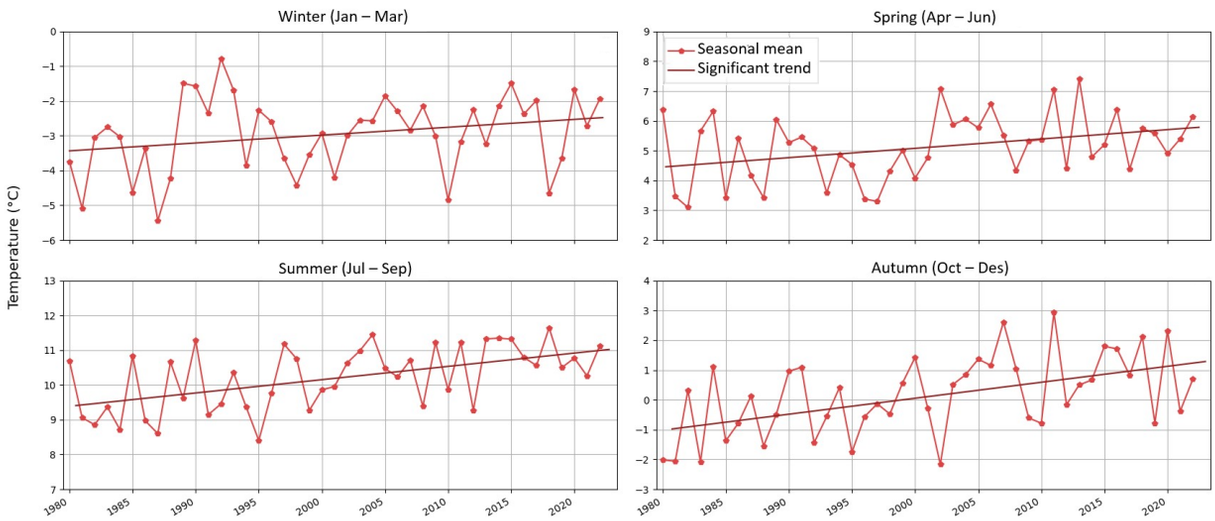

Figure 3.4: Seasonal mean air temperature (^oC) from Tromsø weather station. Solid lines indicate statistically significant trend ($p < 0.05$).

Table 3.1: Seasonal mean temperature (^oC) over the entire study period (1980 - 2022).

Season	Weather station	Mean (^oC)
Winter	Hekkingen fyr	-0.9
	Tromsø	-2.9
Spring	Hekkingen fyr	5.7
	Tromsø	5.1
Summer	Hekkingen fyr	10.7
	Tromsø	10.2
Autumn	Hekkingen fyr	2.2
	Tromsø	0.15

3.1.3 Precipitation

The seasonal mean precipitation at Hekkingen fyr for the period 1980 - 2004 is 224.36, 143.92, 237.37 and 276.15 mm for winter, spring, summer and autumn, respectively (Fig. 3.5). In general most precipitation falls during autumn, however, from 1997 to 2004 there has been more precipitation in winter and summer compared to autumn. Although years where seasonal precipitation exceeds the mean in winter are evenly distributed over the study period, occurrences of seasonal precipitation exceeding 300 mm in winter have been more frequent since 1989. Conversely, for spring and autumn, years where the seasonal precipitation exceeds the mean have decreased with time, while summer

remains relatively unchanged.

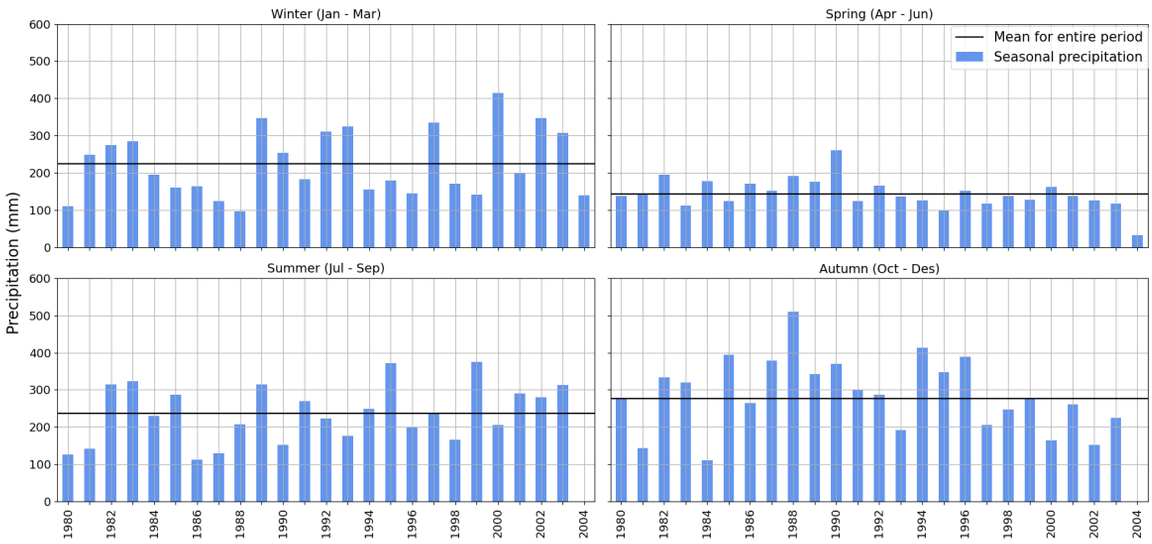

Figure 3.5: Seasonal precipitation (mm) from Hekkingen fyr weather station in the period 1980 - 2004. The black line indicates the seasonal mean for the entire period.

The seasonal mean precipitation for the period 1980 - 2022 at Tromsø weather station is 288.72, 186.51, 265.12 and 336.40 mm for winter, spring, summer and autumn, respectively (Fig. 3.6). For the part of the study period which is covered by Hekkingen fyr (1980 - 2004), overall, precipitation is higher at Tromsø weather station than at Hekkingen fyr. After 2001, both winter and spring experienced more years where the seasonal precipitation exceeds the mean, while autumn saw a decrease. Summer remains relatively unchanged. Winters with seasonal precipitation exceeding 400 mm have become more frequent, with the years 2017, 2019, 2020 and 2021 standing out as a noticeable "cluster" which all exceed 400 mm.

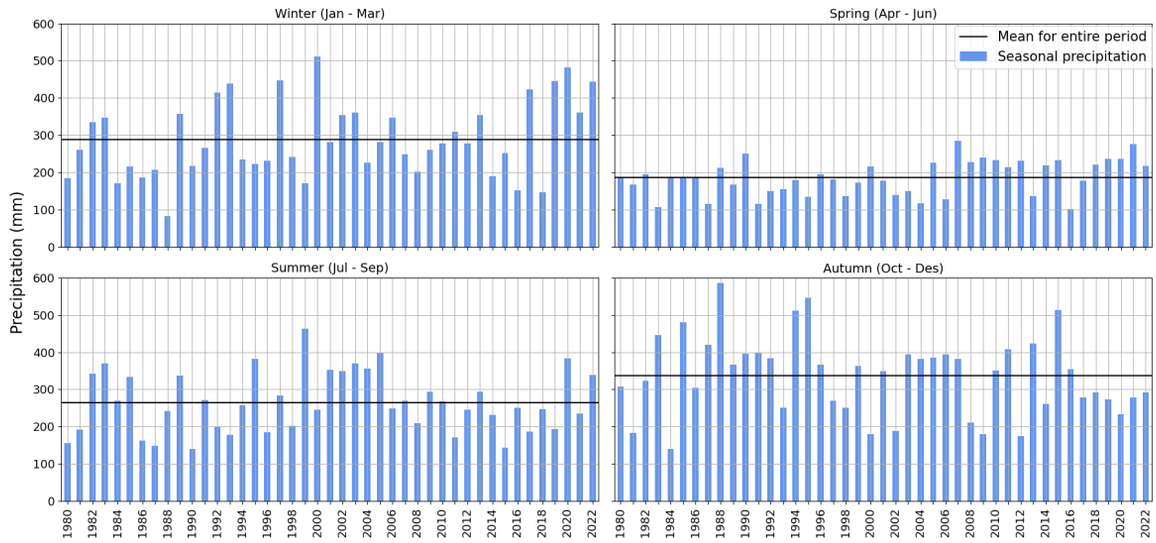

Figure 3.6: Seasonal precipitation (mm) from Tromsø weather station in the period 1980 - 20022. The black line indicates the seasonal mean for the entire period.

3.1.4 River Runoff

Daily runoff from the river Målselva to Malangen is shown in Fig. 3.7. The seasonal pattern of maximum and minimum runoff is clearly visible, with maximum from May to July and minimum from January to March (Fig. 3.7). June 1997 stands out as the only occurrence with runoff over 1400 m^3s^{-1} throughout the observation period. With elevated runoff from mid-May to mid-July, the spring/summer of 2000 is noticeable as well. This coincides with the seasonal winter precipitation in 2000 of about 400 mm, the highest winter precipitation recorded at Hekkingen fyr in the period 1980-2004 (Fig. 3.5). There are also consecutive years with slightly increased runoff in the winter months, such as the period 1990-1993 and 2019-2021, and years where the runoff stays on a moderate level through the peak season, such as 1999 and 2001.

Overall, there is no observable trend in the runoff levels or in the timing of peak discharge throughout the observed period.

The discharge to Balsfjorden from Nordkjoselva displays a similar seasonal pattern to that of Målselva, with maximum runoff in May - July and minimum in January - February (Fig. 3.8). There are no observable changes or trends in the amount of runoff or peak timing, although there are some short periods that stand out with noticeably higher levels, e.g., in January 2002, October 2017

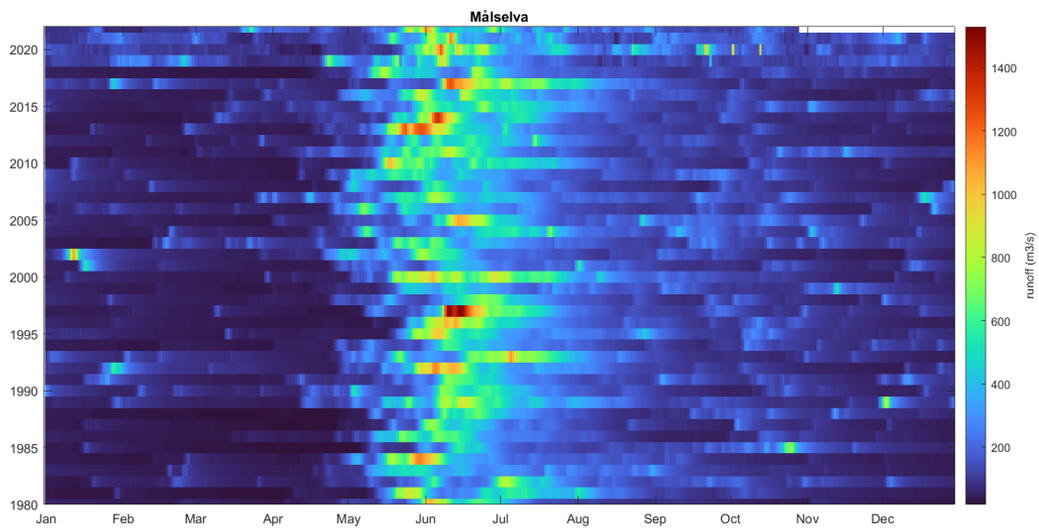

Figure 3.7: Daily runoff (m^3s^{-1}) from the river Målselva to Malangen for the period January 1980 to late October 20222.

and April 2019. These examples are the only registered episodes with daily runoff exceeding 115 m^3s^{-1}. The peaks of June 1997 and May/June 2020 are also noticeable with relatively high runoff. Some of the winter seasons, such as 1981, 1998 and 2018, exhibit abnormally low flow.

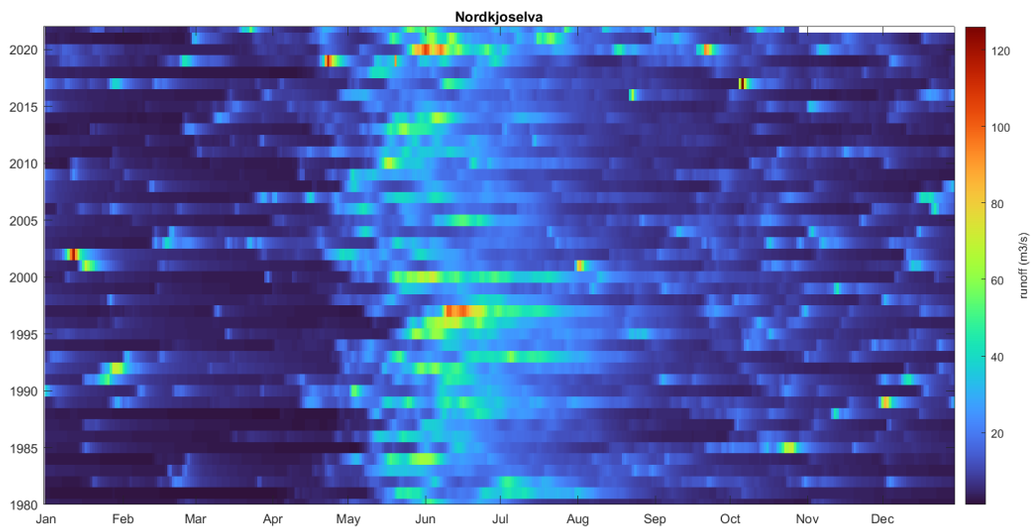

Figure 3.8: Daily runoff (m^3s^{-1}) from the river Nordkjoselva to Balsfjorden for the period January 1980 to late October 2022. Note the colour scale is different from Fig. 3.7.

3.2 Temperature and salinity

In this chapter, a brief summary of the findings regarding temperature and salinity is given, followed by a more detailed description of the results from each fjord.

For Malangen Spildernes, analysis of seasonal temperature reveals that there is a statistically significant, positive trend, in both the surface- and deep layer for all seasons over the observation period (Fig. 3.9). No statistically significant trend is found in the salinity data from Malangen Spildernes. For autumn and spring, the observed warming is largest in the surface layer, while in winter and summer the observed warming is slightly larger in the deep layer.

The temperature data from Balsfjord Svartnes shows a statistically significant, positive trend in both layers across all four seasons as well (Fig. 3.11). As for salinity, there is a statistically significant, negative trend in the spring and summer surface layers, as well as the summer deep layer. Besides these, there are no other statistically significant trends regarding salinity in Balsfjorden. The observed temperature increase is higher in the surface layer than in the deep layer for all seasons.

3.2.1 Malangen

The overall temperature distribution reveals a consistent pattern with distinct layering during the different seasons. In winter, there are two separate layers, where the deep layer is about 2-3 ^oC warmer than the surface layer. As spring arrives, the temperature difference between the two layers diminishes, before two separate layers are again visible in summer. The summer situation is reversed as to that of winter, with the surface layer being 3-4 ^oC warmer than the deep layer. In autumn, the temperature difference again decreases, and the water column is homogeneous in terms of temperature (Fig. 3.9). The seasonal mean temperature in the surface- and deep layer for the entire period is listed in Tab. 3.2.

Through all seasons, the minimum temperature occurred prior to the year 2000, while the maximum temperature occurred after the year 2000 (Tab. 3.2). With an increase of about 2.3 ^oC over the entire observation period, the most pronounced warming of the surface layer has occurred during autumn (Fig. 3.9). The temperature increase for the same period in the winter, summer and spring surface layers is approximately 1.4, 1.3 and 1.15 ^oC, respectively. In the deep layer both winter and summer temperatures have increased with about 1.5 ^oC between 1980 and 2022, while both the spring and autumn temperatures have risen by around 1 ^oC. All trends are statistically significant ($p < 0.05$).

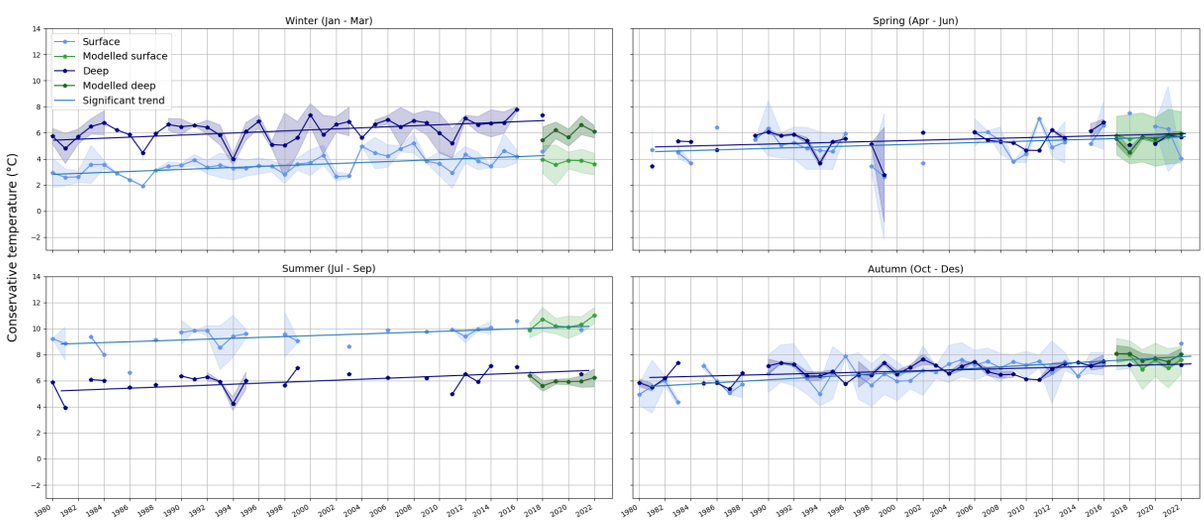

Figure 3.9: Mean seasonal conservative temperature (^oC) in the surface layer (5-6 m) and deep layer (200 m) of Malangen Spildernes. The std is presented as the shaded area around the mean. Blue is CTD data, green is NorFjords160 data. Solid lines indicate statistically significant trend ($p < 0.05$).

Table 3.2: Conservative temperature (^oC) of the surface (5-6 m) and deep (200 m) layers of Malangen Spildernes. Columns show the seasonal mean for the entire study period (1980 - 2022), minimum and maximum, the respective years min/max occurred and the slope of the regression line (bold font for statistically significant).

Season	Layer	Mean	Min	Year$_{min}$	Max	Year$_{max}$	Slope (^{o}C yr^{-1})
Winter	Surface	3.55	1.92	1987	5.19	2008	**0.038**
	Deep	6.16	3.94	1994	7.76	2016	**0.040**
Spring	Surface	5.09	2.62	1999	7.52	2018	**0.028**
	Deep	5.35	2.74	1999	6.75	2016	**0.025**
Summer	Surface	9.38	6.63	1986	10.57	2016	**0.033**
	Deep	5.86	3.88	1981	7.11	2014	**0.038**
Autumn	Surface	6.69	4.33	1983	8.86	2022	**0.055**
	Deep	6.71	5.31	1987	7.60	2002	**0.025**

The overall seasonal pattern in salinity starts off with a winter surface salinity which fluctuates around 33 g kg^{-1} throughout the study period, meaning there is a relatively small difference between the surface and the deep during winter, but still two distinct layers. Salinity stratification increases during spring, most likely depending on the amount and timing of river runoff. This stratification is stable, and strongest, through summer, before the difference between the two layers slightly decreases again over autumn. However, the surface layer salinity is quite variable, meaning there are a few years which deviate from this general pattern. The large variability is also evident in the large standard deviation (Fig. 3.10).

While the past 42 years have revealed substantial changes in the temperature of the Malangen fjord, the changes in salinity are less pronounced. The mean absolute salinity of the deep layer fluctuates between 34 and 35 g kg^{-1} through all four seasons (Fig. 3.10). The only exception is winter 2015, where the mean salinity was 33.7 g kg^{-1}. This is also the lowest deep layer salinity over the time period. The surface layer regression lines all have a negative slope. The winter and autumn deep layer regression lines are slightly negative, while spring and summer are slightly positive. However, none are statistically significant (Tab. 3.3).

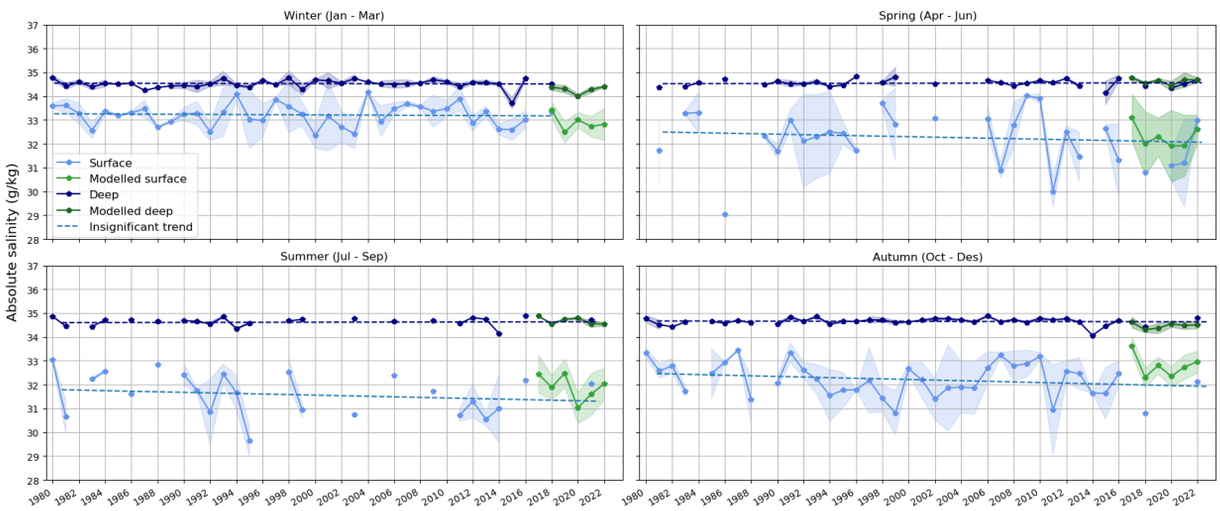

Figure 3.10: Mean seasonal salinity ($g\,kg^{-1}$) in the surface layer (5-6 m) and deep layer (200 m) measured at Malangen Spildernes. The standard deviation is presented as the shaded area around the mean. Blue is CTD data, green is NorFjords160 data. All regression lines (dashed) have P-value > 0.05 indicating there is no statistically significant trend in the data.

Table 3.3: Absolute salinity ($g\,kg^{-1}$) of the surface (5-6 m) and deep (200 m) layers of Malangen Spildernes. Columns show the seasonal mean for the entire study period (1980 - 2022), minimum and maximum, the respective years min/max occurred and the slope of the regression line.

Season	Layer	Mean	Min	$Year_{min}$	Max	$Year_{max}$	Slope ($g\,kg^{-1}\,yr^{-1}$)
Winter	Surface	33.21	32.35	2000	34.16	2004	-0.0024
	Deep	34.52	33.70	2015	34.77	1998	-0.00084
Spring	Surface	32.30	29.04	1986	34.01	2009	-0.013
	Deep	34.54	34.13	2015	34.81	1996	0.00094
Summer	Surface	31.57	29.63	1995	33.03	1980	-0.0117
	Deep	34.61	34.15	2014	34.89	2016	0.00082
Autumn	Surface	32.19	30.80	2018	33.44	1987	-0.013
	Deep	34.65	34.06	2014	34.87	2006	-0.00079

3.2.2 Balsfjorden

The overall pattern in the temperature distribution in Balsfjorden is characterized by distinct layering during the different seasons, however, the pattern differs slightly from that of Malangen. For Balsfjord Svartnes, the winter season is characterized by weak temperature stratification. The two layers hold a similar, and some times overlapping, temperature, but generally the deep

layer is slightly warmer than the surface layer. In spring, the overall pattern appears to be two distinct layers, where the surface layer is warmer than the deep layer, however, there are some years during the observation period where the temperature in the deep layer exceeds the temperature of the surface layer (1998, 2002, 2012), and in 2015 there is an overlap. Through summer, there is further warming of the surface layer, and it holds a temperature which is approximately 4-5 ^oC warmer than the deep layer. In autumn, the layering is again weakened, as the surface layer cools, while the deep layer becomes slightly warmer (Fig. 3.11). The seasonal mean temperature in the surface and deep layer for the entire period is listed in Tab. 3.4.

The largest temperature increase is observed in the surface layer, where, with a difference of about 3 ^oC over the observed period, spring is the season with the most pronounced warming. Followed by autumn, winter and lastly summer, which have had a temperature increase of about 2.7, 1.8 and 1.7 ^oC, respectively. In the deep layer, the largest temperature rise during the observation period is seen in winter, with around 1.4 ^oC increase. Following are summer and autumn, where both seasons show an increase of approximately 1.2 ^oC, while the spring deep layer experiences a temperature increase of about 0.5 ^oC over the same period (Fig. 3.11).

Unlike Malangen Spildernes, the maximum temperatures at Balsfjord Svartnes are not confined to the 2000's; 1992 and 1996 hold the record for maximum temperature in the winter deep- and spring surface layers, respectively (Tab. 3.5). All minima have been measured during the 1980s, apart from the spring surface layer, which had its minimum temperature of 1.98^oC in 1998.

Table 3.4: Conservative temperature (^oC) of the surface (5-6 m) and deep (140 m) layers of Balsfjord Svartnes. Columns show the seasonal mean for the entire study period (1980 - 2022), minimum and maximum, the respective years min/max occurred and the slope of the regression line (bold font for statistically significant).

Season	Layer	Mean	Min	Year$_{min}$	Max	Year$_{max}$	Slope (^{o}C yr^{-1})
Winter	Surface	2.21	0.37	1982	3.80	2008	**0.043**
	Deep	2.92	1.35	1985	4.29	1992	**0.036**
Spring	Surface	4.75	1.98	1998	7.72	1996	**0.071**
	Deep	2.74	0.72	1981	4.11	2012	**0.012**
Summer	Surface	8.28	6.64	1986	11.83	2011	**0.042**
	Deep	2.96	0.97	1981	4.21	2012	**0.029**
Autumn	Surface	5.86	3.74	1983	7.89	2022	**0.064**
	Deep	3.64	1.68	1988	4.82	2014	**0.030**

Figure 3.11: Mean seasonal conservative temperature (^oC) in the surface layer (5-6 m) and deep layer (140 m) measured at Balsfjord Svartnes, with the standard deviation presented as shaded area around the mean. Blue represents CTD data, green represents NorFjords160 data. Solid lines indicate statistically significant trend (p-value < 0.05).

The seasonal pattern is a often homogenous water column in terms of salinity during winter. In spring and summer the difference between the two layers increases, and salinity stratification is stronger, before the difference diminishes over autumn. It is noticeable how much smaller the difference between the surface and deep layer salinity is during winter and autumn in Balsfjorden compared to Malangen. Surface salinity is particularly variable in spring and summer.

The mean deep layer salinity fluctuates between 33 and 34 $g\,kg^{-1}$ through all four seasons (Fig. 3.12) over the observed period. There are a three exceptions: winter 2015 (32.68 $g\,kg^{-1}$), summer 2014 (32.65 $g\,kg^{-1}$) and autumn 2014 (32.63 $g\,kg^{-1}$) which are the minimum salinity measurements of the deep layer for the respective seasons (Tab. 3.5). Besides the autumn deep layer, all regression lines have a negative slope, however only summer is statistically significant.

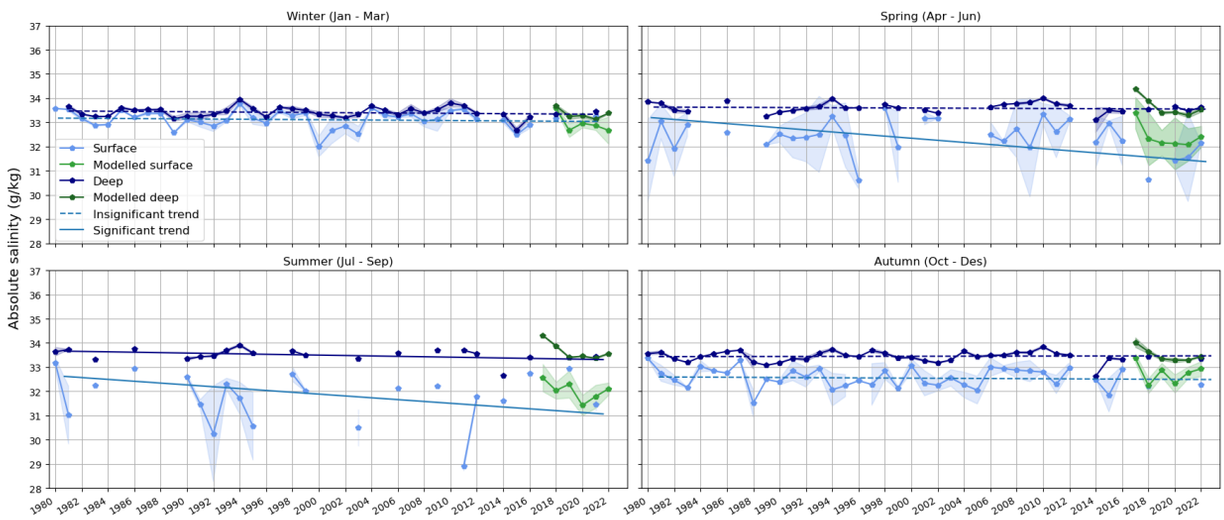

Figure 3.12: Mean seasonal salinity ($g\,kg^{-1}$) in the surface (5-6 m) and deep (140 m) layers, measured at Balsfjord Svartnes. The std is presented as the shaded area around the mean. Blue represents CTD data, green represents NorFjords160 data. Stapled line indicates statistically insignificant trend ($p > 0.05$), solid line indicates statistically significant trend ($p < 0.05$).

Table 3.5: Absolute salinity ($g\,kg^{-1}$) in the surface (5-6 m) and deep (140 m) layers of Balsfjord Svartnes. Columns show the seasonal mean for the entire study period (1980 - 2022), minimum and maximum, the respective years min/-max occurred and the slope of the regression line.

Season	Layer	Mean	Min	$Year_{min}$	Max	$Year_{max}$	Slope ($g\,kg^{-1}\,yr^{-1}$)
Winter	Surface	33.11	31.10	2000	33.78	1994	-0.0034
	Deep	33.40	32.68	2015	33.95	1994	-0.0033
Spring	Surface	32.18	30.60	1996	33.60	1998	**-0.043**
	Deep	33.58	33.10	2014	33.99	2010	-0.0020
Summer	Surface	32.13	28.91	2011	33.17	1980	**-0.038**
	Deep	33.55	32.65	2014	33.91	1994	**-0.0085**
Autumn	Surface	32.55	31.52	1988	33.36	1980	-0.0026
	Deep	33.45	32.63	2014	33.84	2010	0.00078

3.3 Particle tracking simulation

The observed seasonality in river runoff (Chap. 3.1.4) and resulting salinity stratification in spring and summer impact the surface layer dynamics in Malangen and Balsfjorden and the spread of particles brought in by the runoff. The

particle tracking simulations done following maximum spring runoff capture this effect and show the different regional impacts of the rivers in the two fjords.

To gain insight into where the particles end up or accumulate, the study area was divided into four regions (Fig. 2.4). The percentage of particles present in each of these regions, namely Malangen, Balsfjorden, inshore, and offshore (referred to as R1, R2, R3, and R4, respectively), by the end of the simulation was calculated. The results are listed in Tab. 2.4.

Table 3.6: Percentage of particles present in each of the regions by the end of the simulation. For areal coverage of the regions R1 - R4, see Fig. 2.4. The column "other" refers to the percentage of particles which ended up outside of the defined regions.

Year	Source river	R1 Malangen	R2 Balsfjorden	R3 Inshore	R4 Offshore	Sum	Other
2017	Målselva	35	4.5	19	37	95.5%	4.5%
	Nordkjoselva	0	100	0	0	100%	0%
2018	Målselva	46.5	5.5	46.5	0	98.5%	1.5%
	Nordkjoselva	0	87.5	12.5	0	100%	0%
2019	Målselva	21	0	49.5	13	83.5%	16.5%
	Nordkjoselva	9	47	41.5	2.5	100%	0%
2020	Målselva	15.5	4.5	53.5	16	89.5%	10.5%
	Nordkjoselva	0	41.5	58.5	0	100%	0%
2021	Målselva	35.5	1	61	2	99.5%	0.5%
	Nordkjoselva	1	59	40	0	100%	0%
2022	Målselva	1.5	0	78.5	19.5	99.5%	0.5%
	Nordkjoselva	0	54	46	0	100%	0%

3.3.1 Målselva - Malangen

For all simulation years (2017-2022), maximum spring runoff from the river Målselva occurred in June (Tab. 2.1). Discharging into the side-fjord Målselvfjorden, the particles are spread throughout most of Malangen before they leave the fjord, mostly through Rystraumen or the mouth, and occasionally through Gissundet (Fig. 2.2, Fig. 3.13). With varying distributions, the particles are spread along the coast and into the fjords and sounds north of Tromsø (Fig. 3.13). By the end of the 2017 simulation, a slight majority of particles ended up in R4. For 2018, the majority of particles were evenly distributed between R1 and R3, while for the remaining simulations, 2019-2022, the largest accumulation was

in R3 (Tab. 3.6).

In all six simulations, the particle trajectories reveal transport through Rystraumen, but not always into Balsfjorden (Fig. 3.13). For example, in the 2019 (Fig. 3.13c) and 2022 (Fig. 3.13f) simulations, the particles originating from Målselva do not reach further into Balsfjorden than Ramfjorden. The regional distribution after two weeks as shown by percentage of particles per region (Tab. 3.6) also indicate that particles advected into Balsfjorden do not remain there, but are rather transported into the inshore region (R3). The 2017 simulation stands out as the only simulation where there is no transport to the inner part of Malangen, this is also the only simulation year where the majority of particles ended up in R4 (Fig. 3.13a).

The surface salinity implies that river runoff from Målselva does not contribute significantly to the freshwater content in Balsfjorden. On the other hand, fjordwater from Malangen appears to be a source of relatively fresh (< 30 PSU) surface water to the coastal area. The surface salinity also reveals that there are year-to-year variations in the degree of mixing, e.g., when comparing the salinity in the mouth area of Malangen in 2019 (Fig. 3.13c) and 2020 (Fig. 3.13d). In the 2019 simulation, the surface salinity of most of the water in the mouth area is clearly above 27 PSU, while in 2020 it is clearly below.

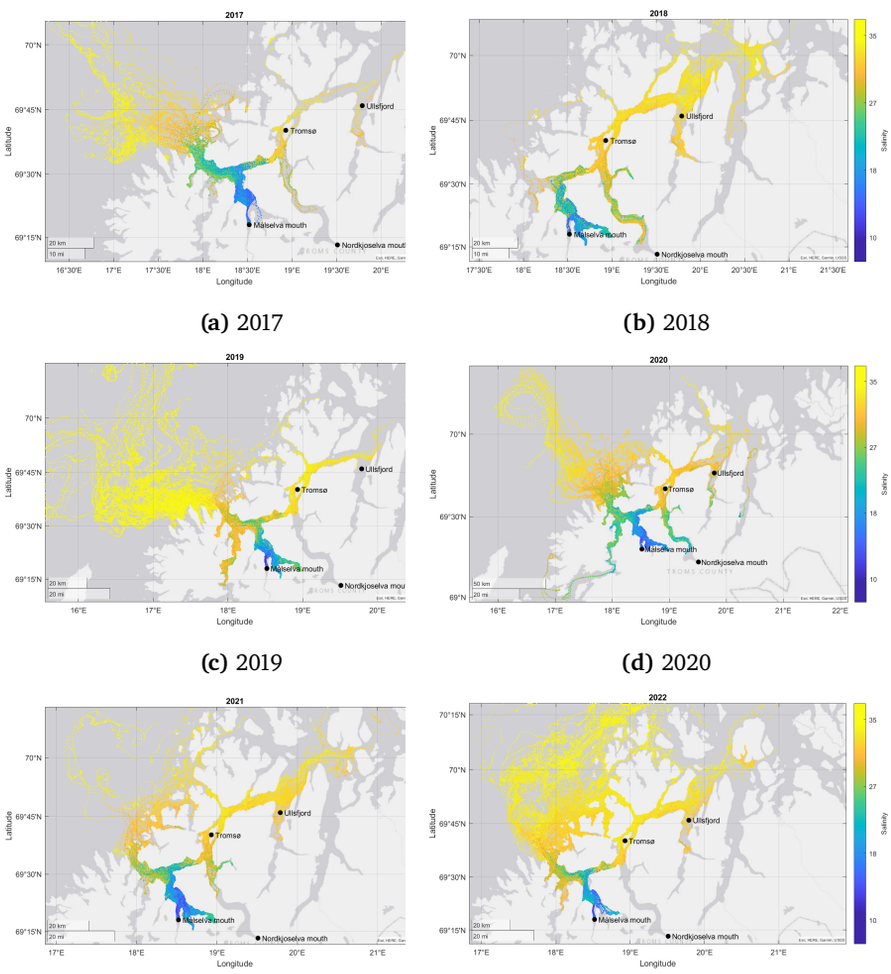

(a) 2017 **(b)** 2018

(c) 2019 **(d)** 2020

(e) 2021 **(f)** 2022

Figure 3.13: Particle distribution 14 days after maximum spring runoff from Målselva 2017 (a) - 2022 (f). Colorbar indicates salinity (PSU) at 1 m depth.

3.3.2 Nordkjoselva - Balsfjorden

For Nordkjoselva, maximum spring runoff for the years 2017 - 2022 occurred between April and June (Tab. 2.1). Nordkjoselva discharges into the inner part of Balsfjorden and how far the particles travel from the source varies from year to year. The most common trajectories are through the fjord, transport into Ramfjorden, and onwards in the north-east direction past Tromsøya. There is little to no transport to the coast. The distribution by region at the end of the simulations reveal that most of the particles originating from Nordkjoselva stay in Balsfjorden (R2), with some transport to R3 as well (Tab. 3.6). In the 2020, 2021 and 2022 simulations (Figs. 3.14d, 3.14e and 3.14f) there is transport into the neighbouring fjord Ullsfjord.

The 2017 and 2019 simulations differ from the overall pattern. In 2017 the particles do not reach further than the entrance to Ramfjorden, making this the only year where 100% of the particles remain in Balsfjorden (Fig. 3.14a). For the 2019 simulation, in addition to being the year with the most significant runoff (Tab. 2.1), it is also the only year which displays advection of Nordkjoselva particles to R4, as well as transport through Rystraumen and into the mouth area of Malangen (Fig. 3.14c).

The surface salinity shows that, generally, the water stays relatively fresh (< 27 PSU) until it reaches Svartnes, gradually becoming more saline as it approaches Tromsøya. The water around Tromsøya generally holds a salinity above 30 PSU.

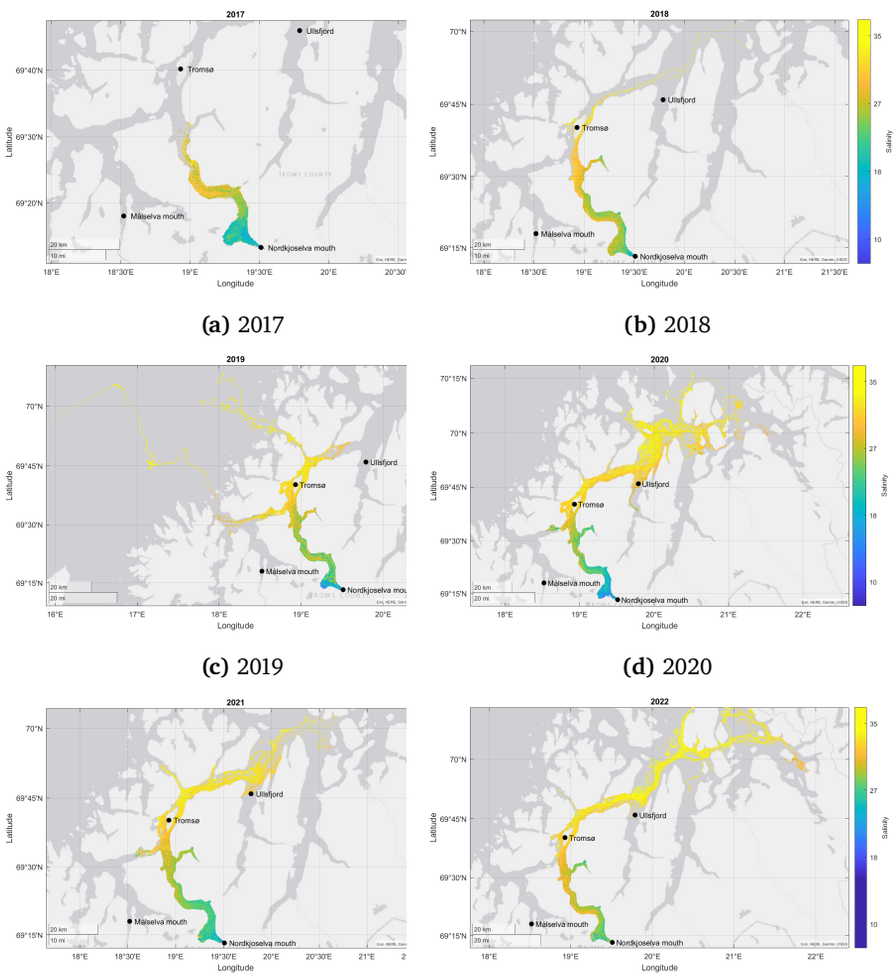

(a) 2017 **(b)** 2018

(c) 2019 **(d)** 2020

(e) 2021 **(f)** 2022

Figure 3.14: Particle distribution 14 days after maximum spring runoff from Nordkjoselva in 2017 (a) - 2022 (f). Colorbar indicates salinity (PSU) at 1 m depth.

4

Discussion

4.1 Hydrography

As described in Chap. 1.1, there are several modes for water exchange between the fjord and the coast. When there is sufficient freshwater input, typically during spring, estuarine circulation will lead to an outflowing current in the surface layer, with an inflowing current at depth. In the intermediate layer, temporal variations in sea level and density at the coast may lead to transport into or out of the fjord. Water exchange between the fjord and the coast leads to exchange of heat and salt, influencing the hydrographic properties of the water masses both in the fjord and at the coast (Sælen, 1950; Aure et al., 1996; Mankettikkara, 2013). A secondary factor which will affect the temperature of the fjordwater is air temperature (Eilertsen and Skarðhamar, 2006). Freshwater supply will mainly contribute to seasonal variations in salinity, affecting stratification, which may lead to more effective heating of the surface layer. These external factors can affect different parts of the water column directly, but through mixing processes, the entire water column may be affected indirectly.

Malangen has a direct and deep connection to the ocean, which enables the inflow of water masses present at the coast. However, it is important to note that Spildernes (the station in Malangen) is located in the inner basin, which is separated from the outer basin by a sill area of about 150 – 160 m depth (Fig. 2.2). This is also a relatively deep and open connection, but still more restricted than the outer basin. Balsfjorden has a more land-locked character,

where the advection of coastal water masses is restricted due to the shallow sills and narrow sounds separating Balsfjorden from the ocean. The deepest, and broadest, connection to Balsfjorden is Rystraumen (50 m deep), hence Balsfjorden will also be affected by water masses from the coast, but most likely via Malangen.

From 1980 until the mid-2000s, observations by IMR show that both the temperature and salinity of the Atlantic Water (AW) along the coast (50 – 200 m depth) has increased. In the more recent years, however, this situation has been reversed, with decreasing temperature and salinity. In 2022, the temperature of the AW was still above the long-term average, while the salinity was slightly below the long-term average at the northern coast (IMR, 2023). Albretsen et al. (2011a) investigated the hydrography of the coastal water (CW) during the winter months in the decade 2000 – 2009. Relative to the reference period 1961 – 1990, the decadal average for the northern stations revealed increased temperature at both 10 and 200 m depth. For the same period, the surface layer displayed decreased salinity, while the deep layer displayed increased salinity. These findings suggest that the properties of the coastal water masses have changed during the study period. The question that arises is whether these changes are noticeable in the fjords.

4.1.1 Temperature

This study finds statistically significant, positive trends in temperature in the surface- and deep layers, through all four seasons in the period 1980 - 2022 in both Malangen and Balsfjorden (Fig. 3.9 & Fig. 3.11). This overall temperature increase is assumed to be a result of mainly two factors. The first factor is the temperature increase in the coastal water masses which has occurred during the same period (Albretsen et al., 2011a; IMR, 2023). Likely, Malangen's deep connection to the coast has allowed for advection of heat from the warming CW and AW, increasing the temperature of the fjordwater. Due to its bathymetry, Balsfjorden will have more exchange in the upper part of the water column, and only limited deep water exchange (Sælen, 1950). Through Rystraumen, Balsfjorden has likely been supplied with CW, and occasionally by AW, however mixed with the fjordwater from Malangen. Due to the shallow depth of Tromsøysundet (8 m) and Sandessundet (11 m), inflow through these sounds may be limited to less dense water, e.g. modified CW and fjordwater.

The second factor which is believed to have affected the temperature in the fjords is air temperature. When examining sea and air temperature data from northern Norway in the period 1980 – 2003, Eilertsen and Skarðhamar (2006) found that the temperature of northern waters is strongly correlated with air temperature. In the present study, we find a statistically significant, positive

trend in air temperature through all four seasons, at both Hekkingen fyr and Tromsø weather stations (Fig. 3.3 & Fig. 3.4). During winter and autumn, the air-water temperature gradient drives conductive heat transfer from the relatively warm water to the colder atmosphere (Turns, 2006). However, as the air temperature during these seasons increases over the study period, the temperature gradient decreases. Consequently, the rate of heat transfer will decrease as well, reducing heat loss from the water during winter and autumn. Conversely, during spring and summer, the direction of heat transfer is reversed, with heat being transferred from the warm atmosphere to the colder water. Increased spring/summer temperatures means the gradient between the air and water will be larger, leading to greater heat transfer from the atmosphere to the ocean.

The warming observed in Malangen for winter and summer over the study period is largest in the deep layer, while the observed warming is largest in the surface layer for spring and autumn. Conversely, the warming observed in Balsfjorden is larger in the surface layer compared to the deep layer, for all seasons. In Malangen, the warming is 0.1 and 0.2 ^oC larger in the deep layer compared to the surface layer for winter and summer, respectively, while the warming in the surface layer is 1.3 and 0.15 ^oC higher than the observed warming in the deep layer for autumn and spring, respectively. These differences may indicate that the external factors which have the largest influence on the temperature in Malangen have a seasonal character. There is seasonality in the inflow of AW, where the "normal" is more inflow to the fjords during summer (Mitchelson-Jacob and Sundby, 2001; Sætre, 2007), coinciding with the larger temperature increase in the deep layer in summer. Further, the largest increase in air temperature at Hekkingen fyr was found during autumn (Fig. 3.3), coinciding with the larger temperature increase in the surface layer during autumn. However, this does not explain the difference during winter and spring. For Balsfjorden, the warming of the surface layer was 0.4, 2.5, 0.5 and 1.5 ^oC greater than the warming of the deep layer for winter, spring, summer and autumn, respectively. The difference is noticeably larger in Balsfjorden compared to Malangen. These findings may indicate that the temperature in Balsfjorden is mainly affected by air temperature, however, there was observed warming in the surface coastal water in the period 2000 - 2009 (Albretsen et al., 2011a), which cannot be ruled out as a potential factor as well.

It is important to point out that the validity of the positive temperature trend in the spring surface layer in Balsfjorden is questioned. The data during spring are limited and highly variable, which is evident from the generally large standard deviation. The estimated trend is calculated from the raw data, while it is presented with the seasonal mean for each year. Due to the large variability, the trend does not, visually, appear to be the best fit to the data, which is further highlighted when comparing it to the (even more limited) summer surface layer

data. The year-to-year variation in magnitude and timing of river runoff likely contribute to the large variability during spring.

4.1.2 Salinity

During the study period the surface CW has gotten fresher, while the deep CW has gotten more saline (Albretsen et al., 2011a; IMR, 2023). The freshening of the coastal surface layer has been attributed to increased precipitation and hence increased runoff along the coast, while the increased salinity in the deeper layers have been attributed to mixing with AW, which has gotten saltier during the same period (Albretsen et al., 2011a; Sætre et al., 2003). However in more recent years, there has been observed decreasing salinity in the AW (IMR, 2023). In the present study, precipitation data from Hekkingen fyr reveals that in the period 1980 – 2004, the frequency of years where the seasonal spring and autumn precipitation was above average decreased with time. Precipitation in summer and winter remained relatively unchanged, however, incidents with seasonal precipitation exceeding 300 mm in winter have been more frequent since 1989. For Tromsø, the time series spans over the entire study period, 1980 – 2022. After 2001, both winter and spring show an increase in years with above-average seasonal precipitation, autumn shows a decrease, while summer has remained relatively unchanged. In other words, there have been seasonal variations in precipitation over the study period, however, no observable trend is found regarding river runoff to neither Malangen nor Balsfjorden. In other words, the trends regarding precipitation and consequently river runoff observed along the coast are not evident locally in Malangen and Balsfjorden. However, even though there is no observable positive/negative trend regarding river runoff, the year-to-year variation will influence the fjords and impact the seasonal signal. The influence of river runoff on the hydrographic properties will be more pronounced in Malangen compared to Balsfjorden, due to the amount of runoff from Målselva being considerably higher than that of Nordkjoselva Tab. 2.1).

In the present study, the surface layer salinity at both locations have displayed high variability throughout the year through the entire study period, especially during the spring and summer seasons. The high variability is evident from the generally large standard deviation, particularly during spring at both locations, but also for the remaining seasons in Malangen. There are no significant trends regarding surface layer salinity in Malangen, while in Balsfjorden both the spring and summer surface layers reveal a statistically significant, negative trend. All regression lines for the surface layer have a negative slope. Conversely, the results regarding deep layer salinity are relatively stable patterns throughout the year in both fjords, during the entire observation period, where the deep layer in Malangen is slightly more saline than the deep layer in Bals-

fjorden. Besides a statistically significant, negative trend in the summer deep layer in Balsfjorden, no statistically significant trends are found regarding deep layer salinity.

Since the surface salinity of the CW has decreased over the duration of the study period, and there has been no discernible trend in river runoff (i.e., decrease), one would expect decreasing surface salinity in the fjord. Although the trends in the surface layer are not significant, the slope of the regression lines are all negative, indicating that the freshening coastal water (in combination with a "normal" runoff pattern) has had an influence on the surface salinity in both fjords.

Furthermore, one would expect to see the changes in the deep layer salinity at the coast reflected in the deep layer of especially Malangen. However, the data from the fjords do not reflect this expectation. There could be several reasons as to why the signal from the coast is not visible in the fjord deep layer. One explanation may be that the fresher surface water has effectively been mixed down in the water column, counteracting the effect of the inflowing, more saline coastal water. Following this argument, it must be emphasized that even though the salinity of the AW has decreased during the recent years, it is still relatively saline compared to the fjord-water.

Another factor to be taken into account is that the inflow of AW will have seasonal variations. Inflow will occur more frequently during summer due to the prevailing northerly wind direction at the coast and following offshore displacement of the surface water due to Ekman transport, allowing inflow of AW into the fjords (Mitchelson-Jacob and Sundby, 2001; Sætre, 2007). The frequency of inflowing AW to the fjord or wind pattern at the coast has not been investigated here, as it is beyond the scope of this study. However, less inflow of AW to Malangen (and by extension Balsfjorden), may also be an explanation as to why the deep layer salinity in the fjords do not reflect the changes in AW salinity.

Lastly, it is also worth considering that the locations of Spildernes and Svartnes may have affected the results, as they are located closer to the river mouths of Målselva and Nordkjoselva than to the fjord mouths. Hence it is possible that the hydrographic patterns from the coast regarding salinity are more visible in the outer part of the fjord, while the signal from the river runoff is more prominent in these stations.

As with the spring surface layer temperature trend in Balsfjorden, the validity of the trends regarding the spring and summer surface salinity in Balsfjorden are questioned. These regression lines have been calculated from the raw data as well, and due to the high variability and limited data, the estimated trend does

not appear to be the best fit when estimating the long-term changes.

4.2 Particle tracking simulations

4.2.1 Particle movement and accumulation

The percentage of particles present in each region by the end of the simulation provides a rough indication of where they end up or accumulate. This is valuable information as the accumulation and spread of particles, such as nutrients, pollutants and planktonic organisms in the fjords surface layer, may affect the fjord-coast ecosystem (see e.g., Frigstad et al. (2020); McGovern et al. (2020)).

Winds have a large impact on the modelled transport of particles in the surface layer (Pedersen et al., 2006; Myksvoll et al., 2012; Skarðhamar et al., 2018). Particles may accumulate in specific areas given a specific, and consistent, wind direction, whereas wind events with considerable strength and variable direction may lead to dispersion (Myksvoll et al., 2012). In the fjord, the wind will most likely be topographically steered either in-fjord or out-fjord, which appears to be the case for both Malangen and Balsfjorden (Fig. 3.1 & Fig. 3.2). At the coast, southerly winds and following onshore Ekman transport will lead to transport into the fjord, while northerly winds and following offshore Ekman transport will lead to transport out of the fjord in the surface layers. Several other factors, such as horizontal density differences, turbulence and the amount of runoff, will also influence the degree of mixing, how far particles travel from the source, and where they accumulate.

Our simulations show that particles originating from Nordkjoselva stay in Balsfjorden (R2), while particles originating from Målselva are transported out of Malangen and into R3 (inshore) (Tab. 3.6), generally spread out over a larger area compared to the Nordkjoselva particles (Fig. 3.13 & Fig. 3.14). From the wind results (Chap. 3.1.1), we saw that the wind speed is generally higher at Hekkingen fyr (Malangen) than in Tromsø (Balsfjorden). Based on the average current speed at Spildernes and Svartnes, calculated from the NorFjords160 results, an estimation of the average time it takes for a particle to travel from the mouth of Målselva/Nordkjoselva to the mouth of Malangen/Balsfjorden was derived. On average, a particle suspended from Målselva in the month of June is estimated to spend approximately 47 hours to reach the coast (about 45 km), hence travelling with a speed of ~ 0.26 m/s. In comparison, a particle suspended from Nordkjoselva during the spring season (Apr-Jun) is estimated to spend about 124 hours to reach the southern tip of Tromsøya (about 59 km), hence travelling with a speed of ~ 0.13 m/s. It is emphasized that this calcula-

tion is an approximation, not an exact measurement, as the complex dynamics of particle movement and varying current speed in different parts of the fjords are not considered. Nonetheless, the calculation implies that the surface currents in Malangen are stronger than in Balsfjorden. The higher surface current speed in Malangen compared to Balsfjorden may be explained by the difference in runoff to the two fjords, where Malangen has a far larger supply than Balsfjorden (Tab. 2.1). The supply of freshwater leads to stronger stratification of the upper parts of the water column, allowing for the wind energy to be concentrated in a relatively shallow layer (Sætre, 2007). Combining this with the generally higher wind speed at Hekkingen fyr vs. Tromsø, may explain the large extent of Målselva particles compared to the relatively small spread of Nordkjoselva particles.

The trajectories show that Målselva particles are transported through Rystraumen eastwards towards Balsfjorden, while Nordkjoselva particles are not transported through Rystraumen westward towards Malangen. The timing of maximum runoff is different between the two fjords. For Målselva, maximum runoff was in June for all simulation years, while for Nordkjoselva the timing of maximum spring runoff was spread out between April and June (Tab. 2.1). However, it is likely that estuarine circulation was already present in Malangen in the years with earlier maximum runoff from Nordkjoselva, as there were peaks in runoff from Målselva coinciding with the timing of maximum runoff from Nordkjoselva (Fig.3.7). The estuarine circulation in Malangen pushes the surface water out of the fjord and into Rystraumen. Therefore, estuarine circulation is a potential explanation as to why particles from Nordkjoselva are hindered from travelling through Rystraumen and into Malangen.

However, there is one simulation, 2019, which displays transport from Balsfjorden through Rystraumen and into Malangen, despite there most likely being stronger estuarine circulation present in Malangen at the time. In this simulation, 9% of the Nordkjoselva particles ended up in R1. In comparison, in 2021 1% ended up in R1, while in the remaining years, no Nordkjoselva particles were present in this region by the end of the simulation (Tab. 3.6). A combination of factors is likely the reason for this exceptional transport, where one factor to be considered is the relatively strong runoff (2019 had the maximum registered runoff from Nordkjoselva among the simulation years). A larger amount of discharge may lead to stronger stratification, and possibly increased surface current speed due to winds. The second is wind direction, more specifically the right wind direction at the right time. Theoretically, if there were upfjord winds with sufficient speed and persistence, coinciding with particles reaching the entrance to Rystraumen, the surface currents would be directed into Rystraumen due to Ekman transport. It is, however, important to note that the resolution of the model may not accurately capture the dynamics in Rystraumen, so further investigation and validation would be necessary to both confirm and describe

the observed particle movement.

4.2.2 Freshwater transport and mixing

From the surface salinity shown in the trajectory maps, it is found unlikely that runoff from Målselva is a source of (relatively) fresh water to Balsfjorden (Fig. 3.13). As the current of river water travels from the river mouth, its salinity increases due to entrainment of more saline water. The eastern part of Rystraumen and the area surrounding Tromsøya contains (surface) water with a salinity higher than 30 PSU, suggesting that the current undergoes further mixing before entering Balsfjorden. The inner part of Balsfjorden is, however, less saline (< 27 PSU), but this is likely due to runoff from Nordkjoselva and other smaller rivers. Additionally, the percentage of Målselva particles that accumulate in Balsfjorden is low, indicating that the surface water from Malangen that does enter into Balsfjorden is transported out of the fjord again northeast past Tromsø, and into neighbouring fjords and sounds in R3. On the other hand, it is found that surface water from Malangen is a source of relatively fresh water (< 30 PSU) to the coastal area.

In the same trajectory maps, year-to-year variations in the degree of mixing is also evident. In the results, a comparison of the surface salinity of the water in the mouth area of Malangen in 2019 and 2022 was exemplified to highlight this. Another example, which further emphasizes the different degrees of mixing, is the surface salinity in Rystraumen, which varies from simulation to simulation. E.g., in the 2020 simulation (Fig. 3.13d) the water originating from Målselva holds a relatively low salinity (<27 PSU) towards the eastern part of Rystraumen, while in the 2022 simulation (Fig. 3.13f), the salinity is above 27 PSU in the middle of Rystraumen, indicating more intense mixing in 2022 compared to 2020. The variation in mixing from year-to-year are likely due to different wind regimes in the different simulations.

4.3 Limitations

Investigating the long-term hydrographic variability in Malangen and Balsfjorden based on CTD data from only two stations (Spildernes and Svartnes) naturally presents limitations. Fjords have large temporal and spatial variability, and the hydrographic signal detected at a single station may not be representative to the fjord as a whole. Furthermore, in years where there is only one measurement over the months defined in the season, the seasonal signal for this year will be based on a single CTD profile. This single profile may not be representative to the hydrographic situation for this specific season, that spe-

cific year. The latter is especially relevant for the spring and summer seasons, due to high temporal variability in runoff.

Since CTD observations represent a snapshot in space and/or time, and model results represent average conditions over a volume continous in time, it is important to note that direct comparison between observations and model results may not always be straightforward (Skarðhamar et al., 2018; Sandvik et al., 2016). Furthermore, the horizontal and vertical resolution limits how well the model can reproduce small-scale processes in fjords and sounds.

Lastly, the results and discussion on particle tracking simulations are based on simulations with a limited release (following maximum spring runoff only), thus the analysis only provides insight on the spring season. Additionally, the particles are held at a fixed depth of 1 m throughout the simulations, hence the analysis does not account for factors such as vertical dispersion and mixing or the effect of stratification on particle dispersion.

Despite these limitations, the analysis is based on data from single stations due to practical restraints such as limited time and resources to analyze the data. The specific stations were chosen, as previously stated, due to their locations being approximately mid-fjord, they are the deepest stations in their respective fjords, and have the largest data availability. Further, it is concluded that the model effectively reproduces the hydrographic conditions based on the available observations, and the results fit well with trends derived from observations, with exception of the trends which have been questioned (both temperature and salinity trends in the spring surface layer and summer surface salinity in Balsfjorden). While acknowledging the limitations, the analysis provides valuable insight to the interannual and seasonal variability of the fjords for the period 1980 - 2022, and the horizontal dispersion of particles and freshwater following spring runoff in the years 2017 - 2022.

5

Summary and conclusion

Analysis of hydrographic time series data from 1980 - 2022 have revealed statistically significant, positive temperature trends for both the surface- and deep layer, all seasons, in both Malangen and Balsfjorden. During the same period, the coastal water masses have experienced an increasing temperature (Albretsen et al., 2011a; IMR, 2023). The present study has revealed statistically significant, positive trends in air temperature through all four seasons at Hekkingen fyr (Malangen) and Tromsø (Balsfjorden) weather stations. Based on these findings, the observed temperature increase in the fjords is attributed to the inflow of warming coastal water masses and increasing air temperature.

The findings regarding deep layer salinity are no statistically significant trends in either fjords, with exception of the summer deep layer in Balsfjorden, which has a statistically significant, negative trend. For surface layer salinity there is a statistically significant, increasing trend for the spring and summer seasons in Balsfjorden, besides these, no trends regarding surface salinity are statistically significant in either fjords. The estimated trends for the surface layer all have negative slopes.

At the coast, the surface CW has gotten fresher, while the deep CW and AW has gotten more saline between 1980 and 2022 (Albretsen et al., 2011a; IMR, 2023). Conversely, in this study, there is found no discernible trend in the amount or timing of river runoff to either of the fjords during the same period. The signal from the coast regarding salinity is not clear in the fjords, and several reasons to why this is have been discussed. Even though the trends in the surface layer

are (mostly) statistically insignificant, they are all negative, indicating that the freshening coastal water, combined with the normal runoff pattern, has had an impact on the surface layer salinity in the fjords. For the deep layer it is hypothesized that effective downward mixing of the fresher surface layer has counteracted the influence of more saline coastal water entering the fjords. Another factor that has been discussed is a change in the frequency of AW intrusion. This is most relevant to Malangen, as it has a deep connection to the coast, whereas Balsfjorden is restricted by shallow sills. Lastly, the closeness between the river mouths and position of the stations that have been investigated, Spildernes and Svartnes, has been discussed as a potential factor.

The findings indicate that the hydrographic properties are affected by climate change, implying a potential for further warming and possibly more prominent changes in salinity. A fresher and warmer surface layer means a less dense surface layer, and hence stronger stratification. Stronger stratification will affect the fjord in several ways; firstly it may lead to decoupled surface layer dynamics, which will enhance surface circulation. Additionally, it may have a negative effect on the ventilation, i.e., carbon and oxygen absorbed in the surface layer will less easily be transported to the deeper parts of the water column (Capotondi et al., 2012).

Particle tracking simulations have provided valuable information on the transport of particles and freshwater. It is observed that most of the particles originating from Målselva are transported out of Malangen and generally spread out along the coast and into the fjords/sounds north of Tromsø, while particles originating from Nordkjoselva mainly stay in Balsfjorden. Given the mixing that occurs as water is transported from Målselva towards Balsfjorden, it is found unlikely that runoff from Målselva contributes with (relatively) fresh water to Balsfjorden. On the other hand, water from Malangen is found to be a source of relatively fresh water to the coast.

5.1 Future work

Consistent data are an important factor when investigating hydrographic variability. Therefore, it is essential that the monitoring in Malangen and Balsfjorden is maintained, preferably at a monthly frequency to capture seasonal variations, alternatively 4-6 times per year combined with high resolution numerical modelling of high quality. Long and consistent observational time series hold significant value, as they enable researchers to assess the impact of climate change and the fjords' response to future climatological and environmental changes.

For future work on this dataset, it is recommended to explore alternative methods for estimating trends. The linear regression has provided valuable information on seasonal trends, but as discussed, with some limitations. This method has shown to not be the best fit for this data, particularly where there are gaps in addition to high variability.

If possible, expanding the analysis to the entire fjord(s), both horizontally and vertically, will yield a more comprehensive understanding of the oceanographic variability and change that has occurred in Malangen and Balsfjorden between 1980 and 2022. For this case, Norfjords160 simulations, covering the entire fjord(s) as well, will be a good supplement to observations. Furthermore particle tracking simulations with flexible depth and release during each of the seasons, would provide information on the seasonal variations of the horizontal and vertical dispersion of particles, in addition to surface currents and mixing.

Lastly, I hope the topics presented in this study will be explored in future research. Among the findings, the observed seasonal difference in warming of the surface- and deep layer of Malangen, in addition to the consistently larger warming of the surface layer compared to the deep layer in Balsfjorden is an interesting result, which hopefully will be examined further. It would be suitable to combine this potential research question with wind observations from the coast and observations/model results of deep layer salinity from the entire Malangen fjord, to also investigate the frequency of AW inflow during the period. Additionally, a comprehensive analysis and comparison of hydrographic changes in other nearby fjords would yield valuable insights on the regional (northern Norway) oceanographic change and variability between 1980 and 2022, as well as the impact of different fjord characteristics to external forcing.

Bibliography

Aksnes, D. L., Aure, J., Johansen, P.-O., Johnsen, G. H., and Vea Salvanes, A. G. (2019). Multi-decadal warming of Atlantic water and associated decline of dissolved oxygen in a deep fjord. *Estuarine, Coastal and Shelf Science*, 228:106392.

Albretsen, J., Aure, J., Sætre, R., and Danielssen, D. S. (2011a). Climatic variability in the Skagerrak and coastal waters of Norway. *ICES Journal of Marine Science*, 69(5):758–763.

Albretsen, J., Sandvik, A. D., Asplin, L., Lien, V. S., and Skardhamar, J. (2022). Norkyst800: versjoner og arkiver—oversikt over versjoner og arkiver av norkyst800 som hittil er brukt for modellering av det fysiske miljø i norsk kystsone-med fokus på implikasjoner for lakselusmodellen til havforskningsinstituttet. *Rapport fra havforskningen*, 35:30. IMR, Bergen, Norway.

Albretsen, J., Sperrevik, A. K., Staalstrøm, A., Sandvik, A. D., Vikebø, F., and Asplin, L. (2011b). Norkyst-800 report no. 1: User manual and technical descriptions. *Fisken og havet*, 2:43. Havforskningsintituttets rapportserie, Institute of Marine Research.

Allen, G. and Simpson, J. (1998). Deep water inflows to upper Loch Linnhe. *Estuarine, Coastal and Shelf Science*, 47(4):487–498.

Asplin, L., Albretsen, J., Johnsen, I. A., and Sandvik, A. D. (2020). The hydrodynamic foundation for salmon lice dispersion modeling along the Norwegian coast. *Ocean Dynamics*, 70:1151–1167.

Aure, J., Molvær, J., and Stigebrandt, A. (1996). Observations of inshore water exchange forced by a fluctuating offshore density field. *Marine Pollution Bulletin*, 33(1):112–119.

Capotondi, A., Alexander, M. A., Bond, N. A., Curchitser, E. N., and Scott, J. D. (2012). Enhanced upper ocean stratification with climate change in the cmip3 models. *Journal of Geophysical Research: Oceans*, 117(C04031).

doi:10.1029/2011JC007409.

Cottier, F., Nilsen, F., Skogseth, R., Tverberg, V., Skardhamar, J., and Svendsen, H. (2010). Arctic fjords: A review of the oceanographic environment and dominant physical processes. *Geological Society of London Special Publications*, 344:35–50.

Cushman-Roisin, B., Asplin, L., and Svendsen, H. (1994). Upwelling in broad fjords. *Continental Shelf Research*, 14(15):1701–1721.

Dalsøren, S. B., Albretsen, J., and Asplin, L. (2020). New validation method for hydrodynamic fjord models applied in the Hardangerfjord, Norway. *Estuarine, Coastal and Shelf Science*, 246:107028.

Darelius, E. (2020). On the effect of climate trends in coastal density on deep water renewal frequency in sill fjords—A statistical approach. *Estuarine, Coastal and Shelf Science*, 243:106904.

Edwards, A. and Edelsten, D. (1977). Deep water renewal of loch etive: A three basin scottish fjord. *Estuarine and Coastal Marine Science*, 5(5):575–595.

Eilertsen, H. C. and Skarðhamar, J. (2006). Temperatures of north Norwegian fjords and coastal waters: Variability, significance of local processes and air–sea heat exchange. *Estuarine, Coastal and Shelf Science*, 67(3):530–538.

Farmer, D. M. and Freeland, H. J. (1983). The physical oceanography of fjords. *Progress in Oceanography*, 12(2):147–219.

Frigstad, H., Kaste, , Deininger, A., Kvalsund, K., Christensen, G., Bellerby, R. G. J., Sørensen, K., Norli, M., and King, A. L. (2020). Influence of riverine input on Norwegian coastal systems. *Frontiers in Marine Science*, 7:332. doi: 10.3389/fmars.2020.00332.

Gade, H. G. and Edwards, A. (1980). *Deep Water Renewal in Fjords*, pages 453–489. Springer US, Boston, MA.

Groß, J. (2012). *Linear Regression*. Lecture Notes in Statistics. Springer, Berlin, Germany. 398pp.

Halbach, L., Vihtakari, M., Duarte, P., Everett, A., Granskog, M. A., Hop, H., Kauko, H. M., Kristiansen, S., Myhre, P. I., Pavlov, A. K., Pramanik, A., Tatarek, A., Torsvik, T., Wiktor, J. M., Wold, A., Wulff, A., Steen, H., and Assmy, P. (2019). Tidewater glaciers and bedrock characteristics control the phytoplankton growth environment in a fjord in the Arctic. *Frontiers in Marine*

Science, 6:254. doi: 10.3389/fmars.2019.00254.

Helland-Hansen, B. and Nansen, F. (1909). The Norwegian Sea: Its physical oceanography based upon Norwegian researches 1900–1904. In Hjort, J., editor, *Report on Norwegian Fishery and Marine Investigation*, volume II. The Royal Department of Trade, Navigation and Industries, Kristiania, Norway. 390pp.

IMR (2022). Strømmodeller. `https://hi.no/hi/forskning/marine-data-forskningsdata/modeller-og-modellering/sirkulasjonsmodeller`. online; accessed 25-May-2023.

IMR (2023). Klimaet ved kysten. `https://www.hi.no/hi/temasider/hav-og-kyst/klimaet-i-havet/klimastatus`. online; accessed 26-May-2023.

Inall, M. and Gillibrand, P. (2010). The physics of mid-latitude fjords: A review. *Geological Society of London Special Publications*, 344:17–33.

Kartverket (2023). Norgeskart, sjøkart. `https://www.norgeskart.no/#!?project=norgeskart&layers=1008&zoom=8&lat=7716487.68&lon=647580.24`. [Online; accessed 16-Febuary-2023].

Mankettikkara, R. (2013). Hydrophysical characteristics of the northern Norwegian coast and fjords. *PhD thesis, Universitetet i Tromsø*. 118pp.

McGovern, M., Poste, A. E., Oug, E., Renaud, P. E., and Trannum, H. C. (2020). Riverine impacts on benthic biodiversity and functional traits: A comparison of two sub-arctic fjords. *Estuarine, Coastal and Shelf Science*, 240:106774.

Mitchelson-Jacob, G. and Sundby, S. (2001). Eddies of Vestfjorden, Norway. *Continental Shelf Research*, 21(16):1901–1918.

Müller, M., Homleid, M., Ivarsson, K.-I., Køltzow, M. A., Lindskog, M., Midtbø, K. H., Andrae, U., Aspelien, T., Berggren, L., Bjørge, D., et al. (2017). Arome-metcoop: A nordic convective-scale operational weather prediction model. *Weather and Forecasting*, 32(2):609–627.

Myksvoll, M., Sandvik, A., Skarðhamar, J., and Sundby, S. (2012). Importance of high resolution wind forcing on eddy activity and particle dispersion in a Norwegian fjord. *Estuarine, Coastal and Shelf Science*, 113:293–304.

Nikolopoulos, A., Skardhamar, J., Zhou, Q., Albretsen, J., and Renner, A. H. H. (2023). Seasonality and variability in circulation patterns in a small sub-arctic fjord. Manuscript in preparation.

NVE - norges vassdrags- og energidirektorat (2023). Hydrologiske data. https://nve.no/vann-og-vassdrag/hydrologiske-data/. online; accessed 23-May-2023.

Pedersen, O., Nilssen, E., Jørgensen, L., and Slagstad, D. (2006). Advection of the red king crab larvae on the coast of North Norway—a lagrangian model study. *Fisheries Research*, 79(3):325–336.

Rinde, E., Bjørge, A., Eggereide, A., and Tufteland, G. (1998). *Kystøkologi-den ressursrike norskekysten*. Universitetsforlaget, Oslo, Norway. 214pp.

Sætre, R. (2007). *The Norwegian Coastal Current: Oceanography and Climate*. Tapir Academic Press, Trondheim, Norway. 159pp.

Sandvik, A. D., Asplin, L., and Skardhamar, J. (2019). Modellering av smittsomme lakseluslarver - bakgrunnsdata for Havforskningsinstituttets modellprodukt til trafikklyssystemet, 2019. *Rapport fra havforskningen*, 53:31. IMR, Bergen, Norway.

Sandvik, A. D., Øystein Skagseth, and Skogen, M. D. (2016). Model validation: Issues regarding comparisons of point measurements and high-resolution modeling results. *Ocean Modelling*, 106:68–73.

Shchepetkin, A. F. and McWilliams, J. C. (2005). The regional oceanic modeling system (roms): a split-explicit, free-surface, topography-following-coordinate oceanic model. *Ocean Modelling*, 9(4):347–404.

Skarðhamar, J., Albretsen, J., Sandvik, A. D., Lien, V. S., Myksvoll, M. S., Johnsen, I. A., Asplin, L., Ådlandsvik, B., Halttunen, E., and Bjørn, P. A. (2018). Modelled salmon lice dispersion and infestation patterns in a sub-arctic fjord. *ICES Journal of Marine Science*, 75(5):1733–1747.

Skarðhamar, J. and Svendsen, H. (2005). Circulation and shelf–ocean interaction off North Norway. *Continental Shelf Research*, 25(12):1541–1560.

Statens kartverk Sjø (2008). *Den norske los: farvannsbeskrivelse. 6. Lødingen og Andenes-Grense Jakobselv*. Navigasjon. Statens kartverk Sjø, Stavanger, Norway, 6 edition. 311pp.

Stigebrandt, A. (2010). Fiord circulation. *Encyclopedia of Ocean Sciences*, pages 353–358.

Stigebrandt, A. (2012). *Hydrodynamics and Circulation of Fjords*, pages 327–344. Springer Netherlands, Dordrecht.

Sælen, O. H. (1950). *The hydrography of some fjords in Northern Norway: Balsfjord, Ulfsfjord, Grøtsund, Vengsøyfjord and Malangen*. Tromsø museum. 92pp.

Sætre, R., Aure, J., and Danielssen, D. (2003). Long-term hydrographic variability patterns off the Norwegian coast and in the Skagerrak. *ICES Mar. Sci. Symp.*, 219:150–159.

Turns, S. (2006). *Thermodynamics: Concepts and Applications*. Cambridge University Press, Cambridge, United Kingdom. 756pp.

Wassmann, P., Svendsen, H., Keck, A., and Reigstad, M. (1996). Selected aspects of the physical oceanography and particle fluxes in fjords of northern Norway. *Journal of Marine Systems*, 8(1):53–71.

Ådlandsvik, B. (2022). LADiM documentation. Release 1.1.0. `https://buildmedia.readthedocs.org/media/pdf/ladim/master/ladim.pdf`. [Online; accessed 08-September-2022].

6

Appendix

6.1 Rotation

Comparing the width of the fjord to the internal Rossby radius (R_i), one can distinguish between narrow and broad fjords. A fjord is narrow if the width $< R_i$, and broad if the width $> R_i$. The rotation of the Earth influences the circulation, particularly if the fjord is classified as broad (Cottier et al., 2010; Cushman-Roisin et al., 1994).

For a two layer system, the internal Rossby radius is given by

$$R_i = \frac{c_i}{f} \tag{6.1}$$

where c_i is the speed of an internal wave and f is the coriolis parameter. c_i is given by

$$c_i^2 = \frac{g' H_1 H_2}{H} \tag{6.2}$$

Where H_1, H_2 is the thickness of the upper and lower layer, respectively, and H is the total depth. g' is reduced gravity, given by

$$g' = \frac{g(\rho_2 - \rho_1)}{\rho_2} \tag{6.3}$$

Where g is the gravitational acceleration, ρ_1 and ρ_2 is the density in the upper and lower layer respectively.

As R_i depends on stratification, the effects of rotation on circulation will vary with season. In a broad fjord, the circulation is deviated to the right (left) by the coriolis force in the northern (southern) hemisphere. As a result, large cross-fjord differences in the temperature and salinity distributions may occur (Wassmann et al., 1996; Cushman-Roisin et al., 1994).

6.2 Comparison of model and observations

Norfjords160 typically reproduces hydrography within one unit for both temperature (difference $< 1\ ^oC$) and salinity (difference $< 1\ \mathrm{g\,kg^{-1}}$). In coastal areas, where there are relatively large gradients, this is considered good (Jofrid Skarðhamar, pers.com.). A more thorough regional evaluation of Norfjords160 using observations from a nearby fjord (Kaldfjorden, approximately 30 km north of Malangen) and from Malangsdjupet has been conducted by Nikolopoulos et al. (2023) (in prep) and confirms that the model adequately captures hydrography and circulation in fjords and on the shelf around Tromsø.

With few exceptions, the model results are within one unit difference from observations of conservative temperature and absolute salinity at both Malangen Spildernes (Fig. 6.1 & Fig.6.2) and Balsfjord Svartnes (Fig. 6.3 & Fig. 6.4). Hence the model is found to successfully reproduce temperature and salinity at the two stations.

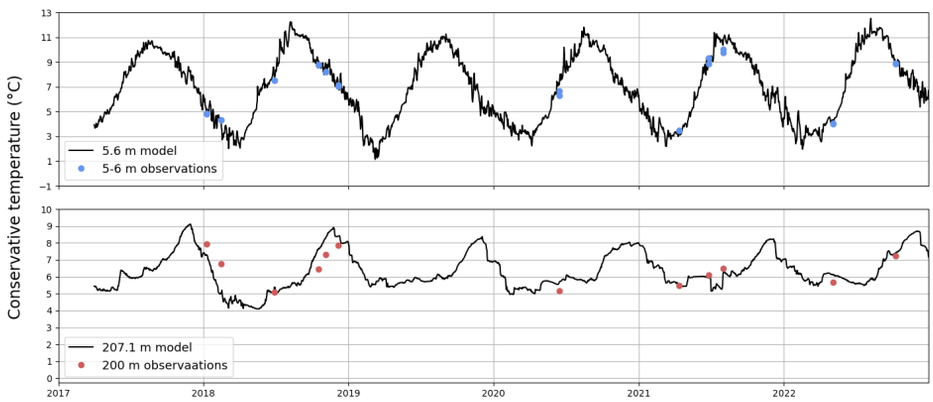

Figure 6.1: Comparison between model results and observations of conservative temperature (^oC) in the surface layer (5-6 m) and the deep layer (200 m) of Malangen Spildernes. Due to the vertical resolution being less dense in the lower part of the water column, the model results for the deep layer are from 207.1 m depth.

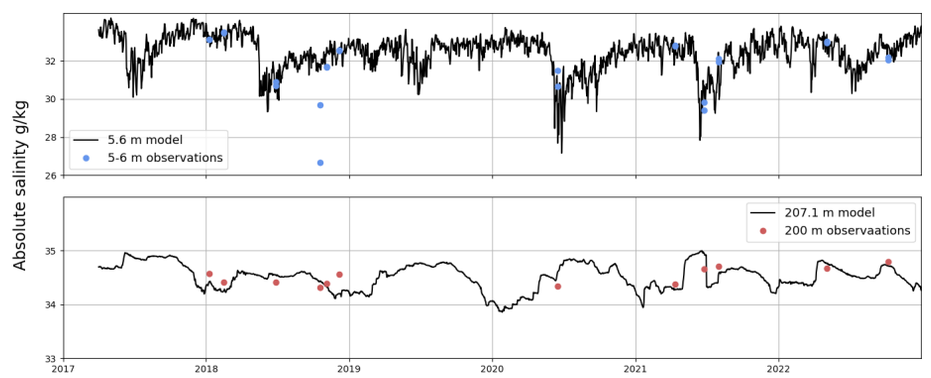

Figure 6.2: Comparison between model results and observations of absolute salinity ($g\,kg^{-1}$) in the surface layer (5-6 m) and the deep layer (200 m) of Malangen Spildernes. Due to the vertical resolution being less dense in the lower part of the water column, the model results for the deep layer are from 207.1 m depth.

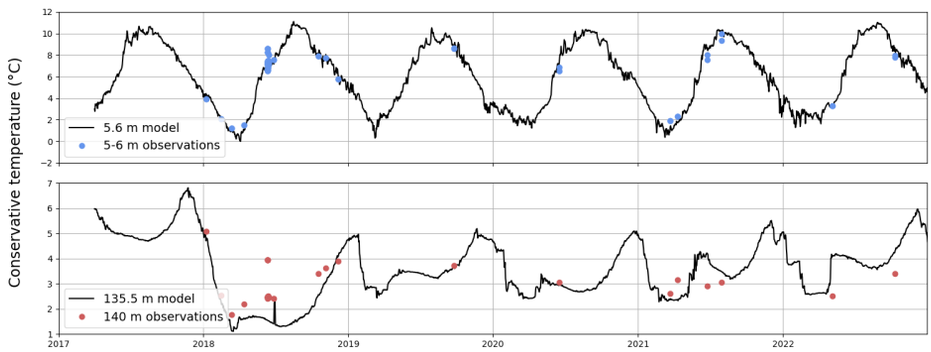

Figure 6.3: Comparison between model results and observations of conservative temperature (^oC) in the surface layer (5-6 m) and the deep layer (140 m) of Balsfjord Svartnes. Due to the vertical resolution being less dense in the lower part of the water column, the model results for the deep layer are from 135.5 depth.

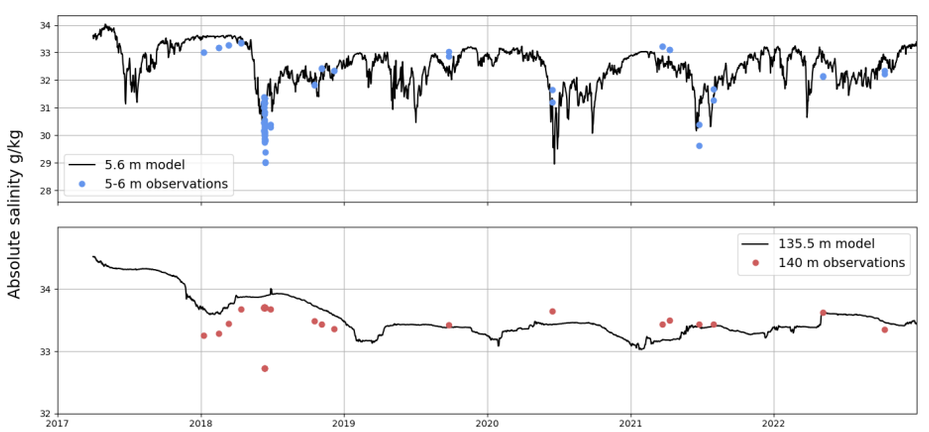

Figure 6.4: Comparison between model results and observations of absolute salinity ($g\,kg^{-1}$) in the surface layer (5-6 m) and the deep layer (140 m) of Balsfjord Svartnes. Due to the vertical resolution being less dense in the lower part of the water column, the model results are from 135.5 m depth.